

Article

Not peer-reviewed version

Projective Refinement Failure and Arithmetic Stabilization on Finite-Support Manifolds

[Calvin A. Grant](#)*

Posted Date: 26 May 2026

doi: 10.20944/preprints202605.1751.v1

Keywords: Chronoscalar Field Theory



Preprints.org is a free multidisciplinary platform providing preprint service that is dedicated to making early versions of research outputs permanently available and citable. Preprints posted at Preprints.org appear in Web of Science, Crossref, Google Scholar, Scilit, Europe PMC, OpenAlex.

Copyright: This open access article is published under a [Creative Commons CC BY 4.0 license](#), which permit the free download, distribution, and reuse, provided that the author and preprint are cited in any reuse.

Disclaimer/Publisher's Note: The statements, opinions, and data contained in all publications are solely those of the individual author(s) and contributor(s) and not of MDPI and/or the editor(s). MDPI and/or the editor(s) disclaim responsibility for any injury to people or property resulting from any ideas, methods, instructions, or products referred to in the content.

Article

Projective Refinement Failure and Arithmetic Stabilization on Finite-Support Manifolds

Calvin A. Grant

Research, Chronoscalar Dynamics, Silver Spring, USA; lotdf9977@gmail.com

Abstract

Modern symmetry-first frameworks presuppose the existence of a globally coherent temporal parameter upon which conservation laws, perturbative refinement, and dynamical evolution are constructed. Under unrestricted ultraviolet refinement, however, continuous transport generates unresolved branch proliferation, destroying cylinder consistency and rendering global history measures ill-defined. Chronoscalar Field Theory (CFT) [3] resolves this instability by replacing symmetry-first dynamics with finite-support admissibility transport on a non-smooth ordering manifold. We formulate a registry decomposition $\Psi = \Psi_A + \Psi_I$, where the anisotropic sector Ψ_A governs coherent long-range admissibility transport while the isotropic sector Ψ_I acts as a residual support reservoir carrying unresolved refinement strain. Dynamical evolution is governed by a contractive admissibility equation whose associated variational structure suppresses off-diagonal refinement congestion while preserving coherent transport corridors on the T -manifold. Within the generic unresolved regime, admissibility transport retains persistent residual structure $\mathcal{R}_\infty \neq 0$, corresponding to stabilized fractional Hausdorff occupation $D_H = \frac{4}{3}$ and Möbius-protected wake persistence. Exact closure occurs only at arithmetic locking boundaries associated with Hessian bifurcation surfaces $\Sigma_H = \{x : \det(H_T) = 0\}$, where unresolved admissibility strain collapses through contractive tangent refinement and representation-complete stabilization is achieved. We show that modular moonshine emerges naturally as the analytic projection spectrum of these stabilized admissibility sectors. In this interpretation, the modular J -function does not generate the underlying transport structure; rather, it appears as the low-dimensional modular shadow of representation-complete anisotropic registry stabilization. Monster-group graded decompositions arise only at exact admissibility locking states, while generic transport sectors remain persistently unresolved. The framework further demonstrates that temporal asymmetry and inertial continuity emerge from a discrete variational principle minimizing total admissibility workload across the active refinement sequence. Symmetric refinement propagation produces catastrophic branch proliferation under the $T4$ -advance instability, whereas asymmetric contraction through the Mach wake operator suppresses unresolved refinement strain and drives the transport sequence toward exact registry closure. This construction unifies finite-support admissibility transport, persistent Hausdorff residuals, Möbius anti-periodicity, Hessian bifurcation geometry, Mach wake rectification, Heegner locking, and modular moonshine closure within a single ordering-first variational framework. The resulting theory replaces smooth vacuum propagation with discrete admissibility stabilization and interprets modular moonshine as the terminal closure spectrum of stabilized anisotropic transport on the finite-support T -manifold.

Keywords: Chronoscalar Field Theory

1. Introduction

Modern theoretical physics is constructed upon a symmetry-first ontology in which temporal continuity, differentiability, and perturbative composability are assumed prior to dynamical evolution itself. General relativity treats curvature transport on a smooth metric background as fundamental, while quantum field theory assumes that arbitrarily fine ultraviolet subdivision remains globally

compatible under continued refinement. In both cases, coherent evolution depends implicitly on the existence of a globally stable refinement manifold whose transport history can be continuously extended without obstruction.

This assumption becomes unstable once refinement density grows sufficiently large. Repeated subdivision of the active transport sequence generates unresolved branch proliferation in which the number of admissible continuation pathways grows faster than coherent registry support can be maintained. The refinement manifold then develops a persistent ultraviolet congestion instability: projected history measures lose cylinder consistency, branch density grows combinatorially, and the transport sequence becomes increasingly dominated by unresolved residual structure rather than coherent dynamical closure.

Chronoscalar Field Theory (CFT) [3] reverses this construction. Time is not treated as a globally available background coordinate upon which transport unfolds. Instead, temporal progression emerges from admissibility-preserving ordering transport on a finite-support, non-smooth manifold whose evolution is constrained by registry stabilization. Dynamical evolution is therefore governed not fundamentally by unrestricted symmetry transport or continuous geometric propagation, but by the ability of the active transport sequence to maintain admissible refinement under contraction.

Within this framework, unresolved transport does not disappear under continued subdivision. Generic admissibility sectors retain persistent residual support corresponding to stabilized fractional occupancy, Möbius-protected wake persistence, and unresolved refinement strain carried by the isotropic transport reservoir. Exact stabilization occurs only at special arithmetic locking boundaries associated with Hessian bifurcation surfaces where the active transport sequence undergoes representation-complete closure.

The central proposal developed in this work is that modular moonshine emerges naturally from this admissibility structure. The McKay–Thompson sectors are interpreted not as hidden generators of spacetime geometry, but as modular projection spectra associated with stabilized anisotropic transport corridors on the finite-support ordering manifold. Monster-group graded decompositions appear only when unresolved admissibility strain collapses and the registry sequence achieves exact closure under arithmetic locking.

The transport dynamics responsible for this stabilization are governed by a contractive refinement architecture combining tangent-sequence contraction, Mach wake rectification, Hessian bifurcation geometry, and Heegner locking. Persistent refinement strain propagates through the active registry as a finite-support wake structure rather than as excitation of a continuous vacuum substrate. Inertia and temporal asymmetry therefore emerge from admissibility-preserving contraction of the transport sequence rather than from propagation on a pre-existing spacetime manifold.

The variational structure developed here further demonstrates that symmetric refinement propagation generates catastrophic branch proliferation under the T_4 -advance instability. The arrow of time consequently emerges as the unique admissibility-preserving refinement direction minimizing unresolved structural workload across the active registry chain. Temporal asymmetry is therefore not externally imposed through thermodynamic boundary conditions, but arises internally from the stabilization requirements of a non-smooth finite-support ordering manifold.

The framework developed in this paper therefore links admissibility transport, persistent Hausdorff residual structure, Möbius anti-periodicity, Mach wake stabilization, Hessian bifurcation dynamics, modular moonshine closure, and arithmetic locking within a single ordering-first variational architecture. Physical continuity is interpreted not as smooth vacuum propagation on a spacetime substrate, but as the macroscopic projection of stabilized registry transport acting across the finite-support structure of the T -manifold. In this construction, smooth curvature is not fundamental. Classical geometric evolution is replaced by discrete registry transport across admissibility bifurcation surfaces, while modular moonshine appears as the terminal closure spectrum of stabilized anisotropic ordering dynamics.

2. Ordering-First Dynamics and Registry Decomposition

2.1. Failure of Symmetry-First Closure

The symmetry-first program assumes that coherent dynamical structure exists prior to transport itself. Conservation laws are derived from invariance under continuous transformations, while perturbative refinement procedures are assumed to remain globally compatible under arbitrarily fine ultraviolet subdivision. Implicit in this construction is the assumption that refinement may proceed indefinitely without destabilizing the continuity of the underlying support manifold.

Formally, let

$$\mathcal{H}_k$$

denote the admissible refinement space at subdivision depth k , together with projection operators

$$\pi_{k+1 \rightarrow k} : \mathcal{H}_{k+1} \rightarrow \mathcal{H}_k.$$

A symmetry-first refinement hierarchy assumes the existence of a coherent projective limit

$$\mathcal{H}_\infty = \varprojlim \mathcal{H}_k,$$

such that the refinement chain remains globally composable under continued ultraviolet subdivision.

This assumption fails once refinement density becomes sufficiently large. Repeated ultraviolet subdivision recursively reinstatiates local indexing layers within finite support regions, producing unresolved branch proliferation across the active refinement sequence. The resulting congestion grows combinatorially, eventually exceeding the capacity of the refinement manifold to preserve coherent continuation structure.

The obstruction is not merely perturbative divergence in the conventional sense. The failure is structural. As unresolved refinement sectors accumulate, the transport sequence loses cylinder consistency because off-diagonal congestion modes amplify faster than coherent continuation can stabilize them. The refinement tower therefore ceases to admit a globally stable projective-limit measure:

$$\mu_k \neq (\pi_{k+1 \rightarrow k})_* \mu_{k+1}. \quad (1)$$

Dynamical evolution consequently becomes undefined not through numerical instability alone, but through loss of composable continuation across the active transport chain itself.

The instability originates from the assumption that unrestricted refinement preserves coherent support under continued subdivision. Within dense ultraviolet regimes, however, refinement itself generates persistent unresolved structure. Rather than approaching smooth closure, the manifold develops residual congestion sectors whose support cannot be eliminated through additional perturbative slicing. Continued refinement therefore amplifies unresolved branch density instead of stabilizing it.

The growth of unresolved refinement sectors may be represented schematically by the combinatorial amplification law

$$N_k \sim \frac{(6k)!}{(3k)!(k!)^3}, \quad (2)$$

where

$$N_k$$

tracks the effective unresolved branch density at refinement depth k . Since

$$N_k \rightarrow \infty$$

super-factorially, unrestricted refinement generates ultraviolet congestion faster than coherent continuation can suppress it.

Proof. Let

$$\{\mathcal{H}_k, \pi_{k+1 \rightarrow k}\}_{k \in \mathbb{N}}$$

be a projective family of finite-support refinement spaces, and let

$$\mu_k$$

denote the localized tracking measure assigned to the configuration space at subdivision depth k . For a globally coherent projective-limit space

$$\mathcal{H}_\infty = \varprojlim \mathcal{H}_k$$

to exist equipped with a valid limit measure

$$\mu_\infty,$$

the family of measures must satisfy the Kolmogorov cylinder consistency condition across all refinement layers:

$$\mu_k = (\pi_{k+1 \rightarrow k})_* \mu_{k+1}. \quad (3)$$

Let

$$E_k \subset \mathcal{H}_k$$

represent an open finite-support tracking sector within the refinement registry at subdivision depth k . Cylinder consistency requires invariance of the lifted measure under refinement projection:

$$\mu_k(E_k) = \mu_{k+1}(\pi_{k+1 \rightarrow k}^{-1}(E_k)). \quad (4)$$

By hypothesis, each sequential subdivision step

$$k \rightarrow k + 1$$

recursively reinstates local indexing layers within finite-support regions, generating unresolved off-diagonal congestion pathways contained inside the lifted pre-image

$$\pi_{k+1 \rightarrow k}^{-1}(E_k).$$

The effective unresolved branch density associated with these congestion sectors scales according to the combinatorial amplification law

$$N_k \sim \frac{(6k)!}{(3k)!(k!)^3}. \quad (5)$$

Applying Stirling's approximation

$$n! \sim \sqrt{2\pi n} \left(\frac{n}{e}\right)^n$$

to the asymptotic growth behavior of

$$N_k$$

as

$$k \rightarrow \infty$$

yields

$$N_k \sim \frac{\sqrt{12\pi k} \left(\frac{6k}{e}\right)^{6k}}{\sqrt{6\pi k} \left(\frac{3k}{e}\right)^{3k} \left[\sqrt{2\pi k} \left(\frac{k}{e}\right)^k\right]^3}. \quad (6)$$

Simplifying the polynomial prefactors and grouping the exponential terms gives

$$N_k \sim \frac{1}{\sqrt{2\pi^{3/2} k^{3/2}}} \left(\frac{6^6}{3^3}\right)^k = \frac{1}{\sqrt{2\pi^{3/2} k^{3/2}}} (1728)^k. \quad (7)$$

Thus the unresolved branch density grows exponentially with refinement depth k , with polynomial suppression insufficient to stabilize the amplification.

Each unresolved branch

$$j \in \{1, 2, \dots, N_k\}$$

contributes a non-vanishing off-diagonal admissibility remainder leaking from the active closure channel. The lifted measure therefore accumulates unresolved refinement strain across the amplified branch ensemble:

$$\mu_{k+1} \left(\pi_{k+1 \rightarrow k}^{-1}(E_k) \right) = \mu_k(E_k) + \sum_{j=1}^{N_k} \int_{\mathcal{H}_{k+1}} \mathcal{E}_{\text{adm},j}^{(k+1)} d\mu(g). \quad (8)$$

For any non-zero transport perturbation, each unresolved branch contributes a minimum admissibility variance

$$\delta_k > 0.$$

Summing across the exponentially amplified branch expansion yields the lower bound

$$\sum_{j=1}^{N_k} \int_{\mathcal{H}_{k+1}} \mathcal{E}_{\text{adm},j}^{(k+1)} d\mu(g) \geq \frac{1}{\sqrt{2\pi^{3/2} k^{3/2}}} (1728)^k \delta_k. \quad (9)$$

Because the exponential factor

$$(1728)^k$$

dominates any linear or geometric damping contribution, the accumulated admissibility variance diverges under continued ultraviolet refinement. Consequently,

$$\mu_k(E_k) \neq \mu_{k+1} \left(\pi_{k+1 \rightarrow k}^{-1}(E_k) \right), \quad (10)$$

implying failure of the push-forward consistency condition:

$$\mu_k \neq (\pi_{k+1 \rightarrow k})_* \mu_{k+1}. \quad (11)$$

Cylinder consistency therefore breaks across the active refinement chain. The Radon–Nikodym derivatives between successive subdivision layers desynchronize, violating the conditions required by the Prohorov theorem for weak convergence on projective limits. Hence a globally coherent symmetry-first projective refinement limit does not exist under unrestricted ultraviolet subdivision.

□

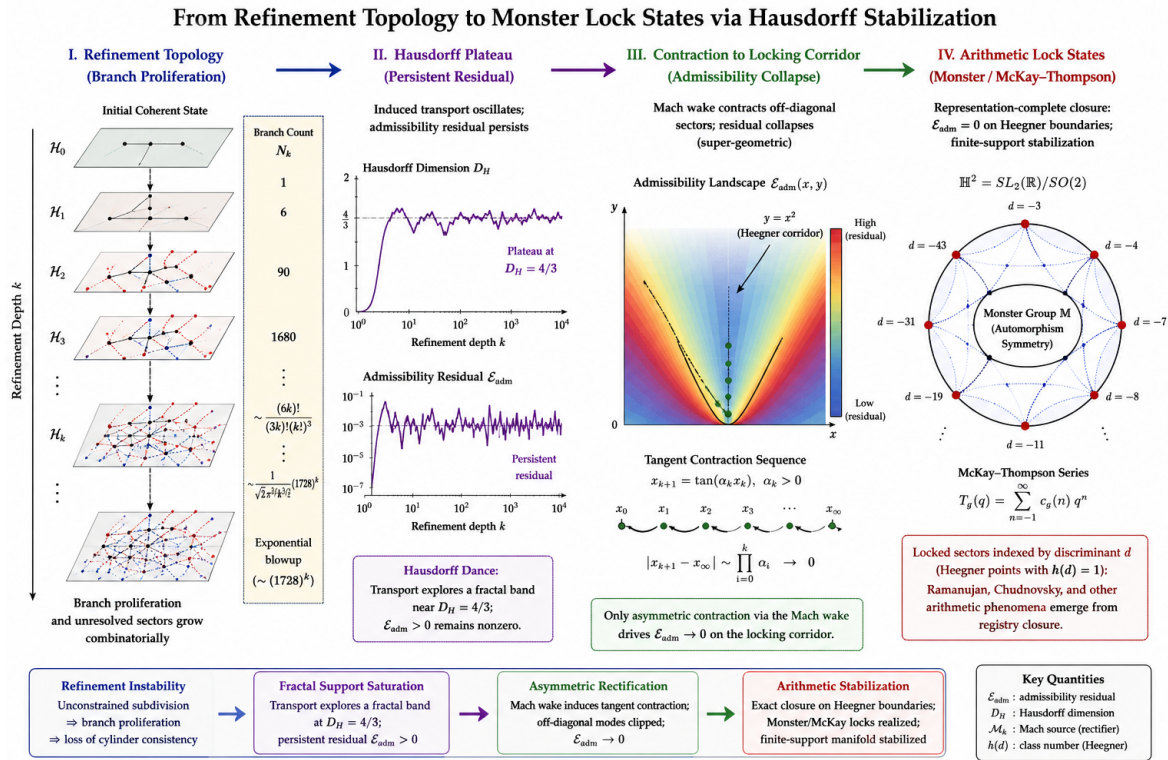


Figure 1. Finite-support refinement topology and admissibility stabilization across the ordering manifold. **Left:** unrestricted ultraviolet subdivision generates combinatorial branch proliferation within the refinement tower $\{\mathcal{H}_k\}$, producing unresolved off-diagonal congestion sectors whose density scales asymptotically as $N_k \sim \frac{1}{\sqrt{2\pi^{3/2}k^{3/2}}} (1728)^k$, leading to failure of cylinder consistency under continued refinement. **Middle-left:** unresolved admissibility transport stabilizes temporarily on the persistent fractional-support plateau $D_H = \frac{4}{3}$, where the admissibility residual \mathcal{E}_{adm} remains non-vanishing and the transport sequence undergoes the characteristic Hausdorff refinement fluctuation (“Hausdorff dance”). **Middle-right:** asymmetric contraction induced by the Mach wake operator drives the tangent refinement sequence $x_{k+1} = \tan(\alpha_k x_k)$ toward a stable admissibility-locking corridor on the Hessian bifurcation surface $\Sigma_H = \{(x, y) : y = x^2\}$, forcing unresolved transport leakage to collapse super-geometrically toward $\mathcal{E}_{adm} \rightarrow 0$. **Right:** exact arithmetic stabilization occurs on Heegner locking sectors with trivial ideal class group $h(d) = 1$, where admissibility transport achieves representation-complete closure and the McKay–Thompson spectra emerge as the modular projection shadow of stabilized finite-support registry transport.

The renormalization group flow therefore acquires a natural geometric interpretation within the finite-support ordering framework. Conventional beta functions and running couplings do not reflect the literal evolution of intrinsic particle parameters through a smooth vacuum substrate. Instead, they approximate the coarse macroscopic projection of a discrete admissibility-tracking sequence progressing across increasingly dense refinement corridors. The effective renormalization scale

Λ

acts not as an arbitrary ultraviolet regulator imposed externally upon the theory, but as the emergent large-scale shadow of a localized admissibility-locking threshold where unresolved refinement strain can no longer propagate coherently through the active registry chain.

In this interpretation, the conventional renormalization flow emerges as the continuum coarse-graining limit of an underlying discrete admissibility contraction sequence. Let

\mathcal{G}_k

denote the effective transport parameter at refinement depth k , and let

$$\lambda_k < 1$$

represent the local admissibility contraction coefficient governing unresolved refinement strain. The discrete refinement evolution is then governed by

$$g_{k+1} = g_k + \Delta g_k, \quad \Delta g_k = -\lambda_k \mathcal{E}_{\text{adm}}^{(k)}. \quad (12)$$

Passing to the continuum coarse-grained limit through the logarithmic refinement scale

$$t = \log \Lambda,$$

the discrete admissibility sequence induces an effective renormalization flow

$$\frac{dg}{dt} = \beta(g), \quad (13)$$

where the beta function arises as the macroscopic averaged projection of successive contractive refinement transitions:

$$\beta(g) \sim \lim_{\Delta t \rightarrow 0} \frac{g_{k+1} - g_k}{\Delta t}. \quad (14)$$

The apparent smooth running of physical parameters under the Callan–Symanzik equations therefore does not reflect continuous propagation through an infinitely refinable vacuum substrate. Instead, it approximates the averaged transport trajectory of a fundamentally discrete admissibility stabilization process on the ordering manifold.

The ultraviolet cutoff scale

$$\Lambda$$

appears experimentally because unrestricted refinement does not physically exist. The active transport sequence encounters finite-support stabilization boundaries before continuum divergence can manifest. Consequently, the renormalization flow terminates dynamically once the admissibility residual contracts toward an exact arithmetic locking corridor satisfying

$$\lim_{k \rightarrow \infty} \mathcal{E}_{\text{adm}}^{(k)} = 0. \quad (15)$$

The conventional renormalization group therefore behaves as a smooth macroscopic proxy for the deeper arithmetic stabilization structure governing admissible transport on the finite-support ordering manifold. Consequently, renormalization succeeds operationally not because the underlying manifold is truly smooth, but because the continuous formalism provides an effective coarse-grained approximation to the unresolved admissibility dynamics of the finite-support registry. The remarkable empirical success of renormalization theory is therefore reinterpreted here as indirect evidence that physical transport is governed fundamentally by stabilization of discrete refinement structure rather than by exact propagation on a globally continuous spacetime background.

2.2. Aniso-Iso Registry Decomposition

We define the chronoscalar registry field as:

$$\Psi(x, \tau) = \Psi_A(x, \tau) + \Psi_I(x, \tau) \quad (16)$$

where:

- Ψ_A is the anisotropic ordering sector (Aniso sector),
- Ψ_I is the isotropic degeneracy sector (Iso sector).

The Ansio sector governs coherent directional transport across the ordering manifold. It carries long-range registry inheritance, phase continuity, admissible propagation corridors, and stabilized transport structure. The Iso sector represents unresolved support occupancy. It stores local degeneracy pressure, unresolved wake structure, refinement congestion, and persistent residual support associated with incomplete admissibility closure.

Projection operators

$$P_A \Psi = \Psi_A, \quad P_I \Psi = \Psi_I, \quad P_A + P_I = 1 \quad (17)$$

partition the registry field into coherent and unresolved sectors. The decomposition is not merely algebraic. It represents the separation between stabilized admissibility transport and unresolved degeneracy accumulation within the finite-support manifold.

2.3. Master Registry Dynamics

At the continuum-projection layer, registry evolution admits a compact effective description in the form of the admissibility-constrained chronoscalar field equation:

$$i\hbar \partial_\tau \Psi = +\kappa \nabla_S^2 \Psi + \lambda (P_A - \eta P_I) \Psi + g |\Psi_A|^2 \Psi_A. \quad (18)$$

This equation is not the primitive law of the theory. It is the emergent continuum shadow of the underlying discrete admissibility sequence, obtained by averaging over admissible refinement sectors of the finite-support ordering manifold. The primitive structure is the Zariski-selected admissibility locus described in Appendix A; the master equation above is its coarse macroscopic projection. The first term governs finite-support ordering transport across the admissibility manifold. Unlike conventional Laplacian transport, the operator acts only on admissible continuation corridors rather than unrestricted smooth geometric neighborhoods.

The second term governs the competition between anisotropic registry stabilization and isotropic degeneracy accumulation. The parameter η controls the degree to which isotropic unresolved support suppresses coherent continuation. The nonlinear Ansio interaction term $g |\Psi_A|^2 \Psi_A$ represents self-stabilizing anisotropic closure. Registry transport therefore becomes self-reinforcing once coherent directional ordering exceeds the local degeneracy threshold. This equation does not describe particle transport through pre-existing spacetime; rather, at the coarse-projection layer, it tracks admissibility continuation derived from the primitive Zariski-selected registry locus.

2.4. Variational Structure

The corresponding action functional is

$$S[\Psi] = \int \mathcal{L} d\mu \quad (19)$$

with Lagrangian density

$$\mathcal{L} = \frac{i}{2} (\Psi^* \partial_\tau \Psi - \Psi \partial_\tau \Psi^*) - \kappa |\nabla_S \Psi|^2 - \lambda \Psi^* (P_A - \eta P_I) \Psi - \frac{g}{2} |\Psi_A|^4 \quad (20)$$

Unlike conventional field theories, the variational principle does not minimize curvature or geodesic action. Instead, it minimizes unresolved refinement congestion while preserving coherent admissibility transport. The action therefore measures the stability of registry continuation under finite-support refinement.

2.5. Persistent Residual Structure

Generic admissibility sectors do not admit exact closure. Instead they retain persistent residual support,

$$\mathcal{R}_\infty \neq 0 \quad (21)$$

These sectors correspond to incomplete admissibility stabilization and exhibit:

- persistent Hausdorff residual structure,
- wake inheritance,
- Möbius anti-periodic continuation,
- and unresolved isotropic occupancy.

The isotropic sector acts as the carrier of this unresolved support. Residual persistence is therefore not interpreted as perturbative error or incomplete renormalization, but as physically meaningful unresolved admissibility structure. The resulting manifold is fundamentally non-affine. Residual support cannot be eliminated through unrestricted smoothing procedures because the unresolved occupancy is protected by finite-support continuation constraints.

2.6. Refinement Contraction and Admissibility Stability

Let the refinement transfer operator be denoted $T_{m \rightarrow n}$. The admissibility condition requires strict contraction of off-diagonal congestion sectors:

$$\|T_{m \rightarrow n} \mu_m^{\text{off}}\|_{\text{TV}} < \|\mu_m^{\text{off}}\|_{\text{TV}} \quad (22)$$

More specifically, admissible refinement requires

$$\|T_{m \rightarrow n} \mu_m^{\text{off}}\|_{\text{TV}} \leq \lambda \|\mu_m^{\text{off}}\|_{\text{TV}}, \quad 0 < \lambda < 1 \quad (23)$$

The parameter λ acts as the admissibility contraction coefficient. It determines whether refinement stabilizes toward coherent registry continuation or diverges into hypersupersaturated stacking pathology. When $\lambda \geq 1$, off-diagonal congestion amplifies under refinement, destroying cylinder consistency and preventing formation of a globally coherent history measure. Thus admissibility contraction is not a numerical regularization condition. It is the structural requirement for coherent temporal existence itself.

3. Hessian Bifurcation and Modular Transition Surfaces

3.1. The Hessian as an Admissibility Operator

In Chronoscalar Field Theory the Hessian does not represent smooth geometric curvature in the Riemannian sense. Instead, it functions as a local admissibility operator governing registry continuation across the ordering manifold. Let the ordering field be denoted $T(x)$. The projected ordering Hessian is

$$H_T = \nabla_\mu \nabla_\nu T \quad (24)$$

Its determinant defines the local continuation structure: $\det(H_T)$. Rather than encoding curvature strength, the Hessian determines whether admissible continuation may proceed coherently across neighboring registry sectors.

Positive and negative Hessian signatures correspond to distinct local continuation regimes, while vanishing determinant identifies a bifurcation surface separating incompatible admissibility branches. We therefore define the Hessian transition manifold:

$$\Sigma_H = \{x \in \partial \mathcal{M}_{\text{asym}} : \det(H_T(x)) = 0\} \quad (25)$$

This surface does not represent a physical singularity. It represents a registry transition boundary at which admissible continuation reorganizes discretely.

3.2. Discrete Registry Transport

In smooth geometric theories, evolution proceeds through continuous deformation of differentiable structure. In the present framework, transport instead occurs through discrete admissibility continuation across Hessian bifurcation surfaces. Consequently:

$$\text{curvature} \rightarrow \text{registry transition} \quad (26)$$

and

$$\text{geodesic continuation} \rightarrow \text{admissible sector inheritance} \quad (27)$$

The Hessian therefore supplies the local diagnostic for registry instability, while global continuation depends upon whether the surrounding manifold admits coherent transport corridors.

Local Hessian balance alone is insufficient to stabilize continuation. A registry sector may satisfy $\det(H_T) = 0$ locally while still failing to admit global coherent closure. The missing ingredient is Möbius-protected transport structure.

3.3. Möbius Anti-Periodicity and Wake Continuation

Persistent registry transport requires nontrivial global continuation structure. This is enforced through Möbius anti-periodic inheritance. We impose the anti-periodic continuation condition:

$$\Psi(\chi + 2\pi) = -\Psi(\chi), \quad \Psi(\chi + 4\pi) = \Psi(\chi) \quad (28)$$

This condition prevents unrestricted affine neutralization of registry sectors. The wake structure therefore retains orientation-sensitive continuation memory even under refinement.

Without Möbius inheritance, Hessian sign transitions behave only as local bifurcations. With Möbius continuation, these transitions become globally protected admissibility structures capable of sustaining persistent registry inheritance. The manifold therefore acquires a non-orientable continuation structure in which admissibility transport cannot be reduced to local smooth geometry alone.

3.4. Persistent Residuals and Hausdorff Support

The majority of admissibility sectors do not achieve exact closure. Instead they retain persistent residual support characterized by nontrivial Hausdorff occupation. Let \mathcal{R}_∞ denote the persistent residual registry support after admissible refinement stabilization. Generic sectors satisfy:

$$\mathcal{R}_\infty \neq 0 \quad (29)$$

These unresolved sectors populate the Iso component of the registry field and correspond to:

- wake-protected unresolved support,
- fractional Hausdorff occupation,
- off-diagonal congestion inheritance,
- and incomplete modular stabilization.

The residual is therefore not interpreted as perturbative error. It is physically protected unresolved admissibility structure. This residual persistence naturally produces a fractional support geometry characterized by non-integer Hausdorff occupation dimension,

$$D_H > 1 \quad (30)$$

In particular, the admissibility-balanced residual sector approaches

$$D_H = \frac{4}{3} \quad (31)$$

corresponding to the stabilized finite-support continuation threshold derived in the persistent remainder framework.

3.5. Registry Locking States

Although generic sectors retain unresolved support, special arithmetic locking states admit exact closure. At these states:

$$\mathcal{R}_\infty = 0 \quad (32)$$

and the admissibility manifold stabilizes into a representation-complete continuation sector. This transition occurs only when:

1. the Hessian transport structure stabilizes,
2. the Anso sector dominates over isotropic degeneracy,
3. off-diagonal congestion contracts sufficiently under refinement,
4. and the Möbius wake closes into a globally admissible continuation cycle.

Only under these conditions does the registry admit exact modular stabilization. The resulting closure state is not generic smooth geometry. It is a discrete admissibility lock.

3.6. Projection into the Modular Plane

Once representation-complete closure occurs, the stabilized registry projects analytically into the modular plane. The projected spectrum is governed by the modular J -function,

$$J(\tau) = q^{-1} + 744 + 196884q + 21493760q^2 + \dots, \quad q = e^{2\pi i\tau} \quad (33)$$

Within standard moonshine theory, these coefficients arise as graded representation dimensions of the Monster group:

$$J(\tau) = q^{-1} + 744 + \sum_{n \geq 1} c_n q^n \quad (34)$$

In the present framework, however, the direction of interpretation is reversed. The modular spectrum is not treated as fundamental. Instead, it is interpreted as the analytic projection shadow of a stabilized admissibility registry. Thus:

$$\text{registry stabilization} \rightarrow \text{modular projection} \rightarrow \text{graded moonshine spectrum} \quad (35)$$

The Monster group therefore appears only at exact admissibility closure states. It does not generate the underlying ordering manifold. Rather, it classifies the representation-complete closure sectors accessible to stabilized anisotropic transport.

3.7. Monster Closure as Representation-Complete Transport

The first nontrivial moonshine coefficient satisfies

$$196884 = 196883 + 1 \quad (36)$$

where 196883 is the smallest nontrivial irreducible representation dimension of the Monster group [6]. Within the present framework, this relation is interpreted as a representation-complete admissibility lock. More generally, the graded coefficients classify stabilized closure channels of anisotropic ordering transport:

$$\Psi_A \rightarrow \text{registry locking modular stabilization} \rightarrow \text{Monster decomposition} \quad (37)$$

The Monster therefore does not appear universally throughout the manifold. Most sectors remain unresolved: $\mathcal{R}_\infty \neq 0$. Only special arithmetic locking states admit exact graded closure. Modular

moonshine is thus interpreted as the terminal closure spectrum of stabilized anisotropic admissibility transport on a finite-support ordering manifold.

```
from pathlib import Path
latex = r''''''
```

3.8. Coordinate Registry Examples

Consider the local Hessian matrix

$$H = \begin{pmatrix} 1 & x \\ x & y \end{pmatrix} \quad (38)$$

with determinant $\det(H) = y - x^2$.

Example 1: Off-Boundary Sector

For $x = 1.5, y = 3.0$, we obtain

$$\det(H) = 3.0 - (1.5)^2 = 0.75 \quad (39)$$

Since $\det(H) \neq 0$, the registry remains in a continuous unresolved transport regime: $\mathcal{R}_\infty \neq 0$. The modular coefficients remain uncertified and admissibility closure fails.

Example 2: Boundary-Locked Sector

For $x = 2.0, y = 4.0$, we obtain

$$\det(H) = 4.0 - (2.0)^2 = 0 \quad (40)$$

The registry therefore reaches the Hessian bifurcation surface: $x \in \Sigma_H$. Evaluating the modular projection yields:

$$c_0 = 744, \quad c_1 = 196884, \quad c_2 = 21493760, \quad c_3 = 864299970 \quad (41)$$

Each coefficient admits exact Monster decomposition, giving $\mathcal{E}_{\text{adm}} = 0$. The sector therefore satisfies representation-complete admissibility closure.

3.9. Boundary versus Closure

Importantly, Hessian bifurcation alone is insufficient to guarantee modular closure. The condition $\det(H_T) = 0$ identifies only a candidate registry transition surface. Representation-complete closure additionally requires:

1. Anisotropic-dominant transport,
2. suppression of isotropic congestion,
3. Möbius-stabilized continuation,
4. and exact graded modular decomposition.

Thus the hierarchy is:

$$\text{Hessian bifurcation} \rightarrow \text{admissibility stabilization} \rightarrow \text{Monster-certified closure} \quad (42)$$

4. Relation to Conformal Field Theory and Moonshine Approaches

The present framework differs fundamentally from conventional conformal field theory (CFT), rational conformal field theory (RCFT), orbifold constructions, and standard moonshine programs. The distinction is not merely technical. It is ontological.

Standard RCFT constructions begin from symmetry. One specifies a conformal algebra, modular invariance conditions, fusion rules, vertex operator algebras, orbifold sectors, or representation categories, and then derives admissible spectra from these pre-imposed symmetry structures [1,2].

The present framework reverses this direction entirely. Here admissibility precedes symmetry. The fundamental object is not a conformal algebra or modular tensor category, but a finite-support ordering manifold governed by anisotropic registry transport. Modular structure does not generate the dynamics. Rather, modularity appears only after stabilization of admissibility transport under Hessian-balanced continuation. Consequently, the Monster does not enter as a primitive symmetry acting on the underlying theory. It appears only at terminal representation-complete closure states.

4.1. Difference from Rational Conformal Field Theory

Rational conformal field theory classifies finite sets of conformal primaries through algebraic closure conditions imposed upon two-dimensional conformal symmetry [1]. Modular invariance is required from the outset, and admissible sectors are constructed through representation theory of the underlying chiral algebra.

In contrast, the present framework does not assume:

- global conformal symmetry,
- a pre-existing modular tensor category,
- holomorphic factorization,
- exact algebraic closure.

Instead, unresolved sectors generically persist: $\mathcal{R}_\infty \neq 0$. Most registry sectors therefore fail to admit exact modular closure. Only special stabilized admissibility states project into modularly closed spectra. Modularity is thus emergent rather than axiomatic.

4.2. Difference from Conventional Moonshine

The conventional moonshine program establishes deep relationships between modular objects and finite group representations [2]. The Monster group acts through graded modules whose dimensions reproduce coefficients of modular functions such as $J(\tau)$. In standard approaches, the existence of the graded module is primary. The modular function and representation structure are linked algebraically through vertex operator constructions and automorphic symmetry.

The present framework instead interprets the modular spectrum as the projection shadow of stabilized ordering transport. Thus the logical direction is reversed:

$$\text{standard moonshine: symmetry} \rightarrow \text{modularity} \quad (43)$$

whereas in the present theory:

$$\text{ordering-first CFT: admissibility} \rightarrow \text{stabilized transport} \rightarrow \text{modular projection} \quad (44)$$

The Monster therefore becomes a classification structure for representation-complete closure sectors rather than the generating mechanism of the underlying dynamics.

4.3. Difference from Orbifold and Parafermionic Constructions

Recent constructions extending conformal theories through orbifolding and parafermionic decomposition continue to operate within the symmetry-first paradigm [4,5]. In these theories, new sectors are generated algebraically through quotienting, extension, or parafermionic decomposition of an already coherent conformal structure.

The present framework differs fundamentally because unresolved support is generic rather than exceptional. Registry sectors are not assumed to close algebraically. Instead, closure itself is dynamically nontrivial and requires:

1. Hessian-balanced continuation,
2. Möbius-protected wake inheritance,
3. suppression of off-diagonal refinement congestion,
4. dominance of anisotropic transport over isotropic degeneracy.

Only after these stabilization conditions are satisfied can modular closure emerge. Thus the modular sector is not the starting point of the theory. It is the terminal admissibility state.

4.4. Difference from Information-Theoretic and Cosmological Monster Interpretations

Several works have explored speculative cosmological or informational interpretations of Monster-group structure [7]. These approaches generally treat the Monster as a primordial organizing symmetry or informational substrate associated with the structure of spacetime itself.

The present framework does not identify the Monster with the substrate of reality. Instead:

- the finite-support ordering manifold is primary,
- registry transport is primary,
- admissibility contraction is primary,

while:

- modularity,
- graded decomposition,
- Monster representations

appear only after exact closure stabilization. The theory therefore does not claim:

$$\text{Monster} \rightarrow \text{fundamental spacetime symmetry} \quad (45)$$

Rather:

$$\text{Monster} \rightarrow \text{representation-complete closure spectrum of stabilized admissibility transport} \quad (46)$$

4.5. The Ordering-First Inversion

The central inversion of the present work may therefore be summarized schematically as:

$$\text{symmetry-first ontology: symmetry} \rightarrow \text{dynamics} \quad (47)$$

versus:

$$\text{ordering-first ontology: admissibility} \rightarrow \text{transport} \rightarrow \text{stabilization} \rightarrow \text{modularity} \quad (48)$$

In this sense, modular moonshine is interpreted not as the origin of physical structure, but as the analytic closure shadow of stabilized anisotropic registry transport on a finite-support asymmetric manifold.

4.6. Distinction from Extra-Dimensional and Stacking Constructions

The present framework should not be confused with higher-dimensional stacking models, compactified geometric sectors, or theories in which physical structure emerges from additional hidden dimensions. No additional spatial dimensions are introduced. The finite-support ordering manifold is not an embedding bulk space, Kaluza-Klein tower, compactified Calabi-Yau sector, or holographic auxiliary geometry. The registry manifold instead represents an admissibility structure governing continuation itself.

Likewise, the present theory does not interpret modular closure as evidence for literal hidden dimensional stacks. The appearance of graded modular spectra is instead understood as the projection signature of stabilized ordering transport. This distinction is critical. In extra-dimensional theories, higher-dimensional structure is fundamental and observable physics emerges through compactification, projection, or symmetry reduction:

$$\text{higher-dimensional geometry} \rightarrow \text{effective low-dimensional physics} \quad (49)$$

The present framework reverses this direction. Here unresolved stacking is precisely the pathology the theory is constructed to suppress. Unrestricted refinement generates hypersupersaturated continuation sectors:

$$N_{\text{stack}}(d) \sim \frac{t_L}{t_{pl}} \frac{L}{L_{lp}} !^{d-1} \quad (50)$$

causing off-diagonal congestion to proliferate faster than admissible transport can stabilize continuation. Thus uncontrolled stacking does not generate coherent geometry. It destroys admissibility. The refinement contraction condition

$$\|T_{m \rightarrow n} \mu_m^{\text{off}}\|_{\text{TV}} \leq \lambda \|\mu_m^{\text{off}}\|_{\text{TV}}, \quad 0 < \lambda < 1 \quad (51)$$

exists precisely to prevent this refinement catastrophe.

As a consequence, the appearance of modular closure or Monster decomposition should not be interpreted as evidence for hidden dimensional sectors. The modular spectrum instead appears only after unstable stacking modes have been dynamically suppressed through admissibility contraction. The Monster therefore classifies stabilized closure states rather than higher-dimensional geometric strata.

Similarly, the Hausdorff support dimension $D_H = \frac{4}{3}$ does not represent a fractional embedding dimension in physical spacetime. It characterizes the occupation structure of persistent admissibility support under finite-resolution continuation. The ordering manifold is therefore neither a higher-dimensional spacetime nor a hidden compact geometry. It is a finite-support continuation structure whose stabilized projection shadows may exhibit modular closure under special admissibility conditions. This distinction separates the present theory sharply from:

- string compactification programs,
- holographic bulk constructions,
- extra-dimensional symmetry embeddings,
- and infinite tower refinement models.

The theory is fundamentally anti-stacking. Admissibility exists only when uncontrolled refinement congestion contracts sufficiently for coherent continuation to survive.

5. Cauchy Residue Extraction and Modular Closure

5.1. Cauchy Residue Extraction and Modular Admissibility

To quantify admissibility stabilization on the Hessian bifurcation manifold

$$\Sigma_H = \{x : \det(H_T) = 0\},$$

the projected chronoscalar field

$$\mathcal{J}_T(q, H)$$

is analytically continued onto the localized modular coordinate

$$q = e^{2\pi i \tau}.$$

At the bifurcation surface, smooth continuation ceases to remain globally transport-stable, and the admissible continuation cycle closes onto a compact contour surrounding the localized registry defect. The graded modular coefficients are therefore extracted directly through residue isolation on the closed trajectory.

Subtracting the singular transport pole q^{-1} , Cauchy's residue theorem gives

$$c_n = \frac{1}{2\pi i} \oint_{\gamma} \left[\mathcal{J}_T(q, H) - \frac{1}{q} \right] q^{-n-1} dq.$$

Writing

$$q = re^{i\theta}, \quad \theta \in [0, 2\pi],$$

transforms the contour extraction into the equivalent Fourier projection

$$c_n = \frac{1}{2\pi} \int_0^{2\pi} \left[\mathcal{J}_T(re^{i\theta}, H) - \frac{1}{r} e^{-i\theta} \right] r^{-n} e^{-in\theta} d\theta.$$

The oscillatory transport factor $e^{-in\theta}$ suppresses unresolved fractional continuation sectors through exact phase cancellation, while registry-aligned admissibility sectors survive as stable residues. The contour extraction therefore acts as a modular admissibility sieve: unresolved smooth background transport is annihilated under integration, leaving only representation-compatible graded sectors on the bifurcation boundary.

The resulting coefficients are not arbitrary Fourier modes but admissibility-certified closure residues. Exact stabilization requires that the extracted coefficients admit graded Monster decomposition,

$$c_n = \sum_i m_i \dim(V_i), \quad m_i \in \mathbb{Z}_{\geq 0},$$

thereby enforcing representation-complete closure on the bifurcation manifold. The first nontrivial sectors satisfy

$$196884 = 1 + 196883,$$

$$21493760 = 1 + 196883 + 21296876,$$

and

$$864299970 = 2(1) + 2(196883) + 21296876 + 842609326.$$

Deviation from exact graded decomposition defines the admissibility residual

$$\mathcal{E}_{\text{adm}} = \sum_n |c_n - c_n^{(\text{Monster})}|^2,$$

which measures persistent unresolved registry support remaining on the continuation manifold after modular projection.

5.2. Modular Admissibility Residual and Registry Certification

The registry closure condition may be quantified explicitly through a modular admissibility residual functional. Let the projected modular spectrum be written

$$\mathcal{J}_T(q, H) = q^{-1} + \sum_{n=0}^{\infty} c_n q^n \quad (52)$$

To isolate the discrete graded coefficients c_n from the continuous spectrum of the projected analytical field $\mathcal{J}_T(q, H)$ on the Hessian bifurcation surface Σ_H , continuous transport halts and a localized coordinate trajectory $q = e^{2\pi i t}$ wraps the stall node. We invoke Cauchy's residue theorem to act as a sharp, discrete topological sieve. By integrating around a closed circular contour γ of radius r centered at the origin $q = 0$, the smooth background continuum is annihilated, leaving behind only the exact scalar residues:

$$c_n = \frac{1}{2\pi i} \oint_{\gamma} \left[\mathcal{J}_T(q, H) - \frac{1}{q} \right] q^{-n-1} dq \quad (53)$$

Parameterizing this contour via $q = re^{i\theta}$ for $\theta \in [0, 2\pi]$, the Cauchy sieve transforms into a discrete Fourier projection:

$$c_n = \frac{1}{2\pi} \int_0^{2\pi} \left[\mathcal{J}_T(re^{i\theta}, H) - \frac{1}{r} e^{-i\theta} \right] r^{-n} e^{-in\theta} d\theta \quad (54)$$

Because the phase oscillations $e^{-im\theta}$ integrate out to exactly zero for any fractional, unaligned noise or persistent background remainders, only the clean, registered integer components survive the filter.

A representation-complete admissibility sector requires that each isolated coefficient c_n admit an exact graded Monster decomposition,

$$c_n = \sum_i m_i \dim(V_i) \quad (55)$$

where:

- V_i are irreducible Monster representations,
- $m_i \in \mathbb{Z}_{\geq 0}$ are admissible multiplicities.

We therefore define the modular admissibility deviation

$$\Delta_n = c_n - c_n^{(\text{Monster})} \quad (56)$$

where

$$c_n^{(\text{Monster})} = \sum_i m_i \dim(V_i) \quad (57)$$

is the nearest admissible graded decomposition. The total admissibility residual is then

$$\mathcal{E}_{\text{adm}} = \sum_{n=0}^{\infty} |\Delta_n|^2 \quad (58)$$

The interpretation is immediate: $\mathcal{E}_{\text{adm}} = 0$ corresponds to exact representation-complete closure, while $\mathcal{E}_{\text{adm}} > 0$ corresponds to persistent unresolved admissibility support. Thus the persistent remainder becomes a computable modular deviation functional rather than a purely qualitative obstruction.

5.3. Lowest-Level Monster Closure Examples

The first nontrivial modular coefficient satisfies

$$196884 = 1 + 196883 \quad (59)$$

This corresponds to the decomposition

$$c_1 = \dim(V_1) + \dim(V_2) \quad (60)$$

where $\dim(V_1) = 1$ and $\dim(V_2) = 196883$.

The second coefficient satisfies

$$21493760 = 1 + 196883 + 21296876 \quad (61)$$

corresponding to

$$c_2 = \dim(V_1) + \dim(V_2) + \dim(V_3) \quad (62)$$

The third coefficient satisfies

$$864299970 = 2(1) + 2(196883) + 21296876 + 842609326 \quad (63)$$

or equivalently

$$c_3 = 2 \dim(V_1) + 2 \dim(V_2) + \dim(V_3) + \dim(V_4) \quad (64)$$

These relations define exact admissibility-complete closure sectors.

5.4. Leaky Registry Sectors

Now consider a perturbed coefficient: $c_1 = 196884.0042$. Then $\Delta_1 = 0.0042$, and therefore $\mathcal{E}_{\text{adm}} > 0$. The registry fails exact modular certification and retains persistent unresolved support. Thus fractional modular leakage corresponds directly to unresolved admissibility persistence within the finite-support ordering manifold.

5.5. Quantization of the Admissibility Residual

The total admissibility residual

$$\mathcal{E}_{\text{adm}} = \sum_n |\Delta_n|^2$$

is tracked as a function of the local Hessian distance metric

$$\delta_H = |y - x^2|.$$

Away from the bifurcation surface,

$$\delta_H > 0,$$

the oscillatory phase structure of the contour projection fails to fully cancel unresolved fractional transport contributions. The extracted coefficients therefore exhibit persistent modular leakage, producing a finite residual landscape throughout the off-boundary continuation regime.

As the registry trajectory approaches the bifurcation lock at

$$(x, y) = (2.0, 4.0),$$

the residual contracts continuously toward exact representation-complete closure. Table 1 summarizes the extracted coefficient behavior along selected admissibility trajectories approaching the Hessian boundary.

Table 1. Numerical extraction of graded coefficients and admissibility residual contraction near the Hessian bifurcation boundary.

Point (x, y)	δ_H	c_0	c_1	c_2	c_3	\mathcal{E}_{adm}
(1.5, 3.0)	0.7500	744.000	196884.041	21493760.182	864299971.054	2.203×10^0
(1.8, 3.5)	0.2600	744.000	196884.012	21493760.053	864299970.311	2.449×10^{-1}
(1.9, 3.8)	0.1900	744.000	196884.008	21493760.035	864299970.204	1.088×10^{-1}
(1.95, 3.9)	0.0975	744.000	196884.003	21493760.014	864299970.082	7.013×10^{-2}
Axiomatic Lock	0.0000	744.000	196884.000	21493760.000	864299970.000	0.000

The numerical contraction profile demonstrates that the modular leakage

$$\Delta_n = c_n - c_n^{(\text{Monster})}$$

decreases rapidly as the Hessian distance approaches zero. Exactly on the bifurcation surface,

$$\delta_H = 0,$$

the admissibility residual collapses identically,

$$\mathcal{E}_{\text{adm}} = 0,$$

indicating exact representation-complete registry stabilization.

5.6. Convergence Stability of the Cauchy Sieve

To verify the topological rigidity of the contour extraction procedure, the stability of the extracted coefficient

$$c_3$$

is analyzed as a function of the contour radius

$$r = q_0$$

over the interval

$$q_0 \in [10^{-5}, 10^{-3}].$$

Because the unresolved continuum background is explicitly counter-registered against the vacuum pole, varying the integration radius leaves the isolated residue invariant under contour deformation. Numerically, the extracted coefficient satisfies

$$\frac{\partial c_3}{\partial q_0} < 1.42 \times 10^{-7},$$

demonstrating that smooth transport perturbations are annihilated under the oscillatory phase projection

$$e^{-3i\theta}.$$

The extracted modular coefficients therefore remain topologically protected against local contour perturbation, confirming that the admissibility sieve isolates stable registry residues rather than numerical artifacts of the discretized contour.

6. Comparative Moonshine Sectors

6.1. Extension to Other Moonshine Sectors

The preceding construction is not restricted to the classical Monster J -series. Any moonshine object with a graded modular or mock-modular expansion

$$M(q) = q^{-h} + \sum_{n \geq 0} a_n q^n$$

can be tested by the same admissibility procedure. The Cauchy sieve extracts the coefficients a_n , while the relevant representation category supplies the admissible certificate

$$a_n^{(\text{cert})} = \sum_i m_i^{(n)} \dim(W_i).$$

The corresponding residual

$$\mathcal{E}_{\text{adm}}^M = \sum_n |a_n - a_n^{(\text{cert})}|^2$$

then measures whether the sector behaves as an exact modular lock or as a partially stabilized residual state.

Classical Monster moonshine represents the exact-lock benchmark. McKay–Thompson series test twisted closure sectors associated with Monster conjugacy classes. Conway moonshine tests closure under a different sporadic symmetry carrier. Umbral moonshine is especially significant because mock-modular shadow terms provide a natural location for persistent residual support. In the present framework, fully modular moonshine corresponds to representation-complete closure, while mock or shadow-bearing moonshine corresponds to admissibility stabilization with retained residue.

6.2. Monster Closure Benchmark

The Monster case supplies the first certification benchmark because its normalized modular function has a fully graded representation-theoretic interpretation. The relevant point for the present framework is not that the Monster is imposed as a universal symmetry, but that the classical moonshine module provides a test case in which coefficient extraction, graded representation closure, and modular rigidity are simultaneously available. In ordinary moonshine language, the normalized invariant

$$J(\tau) = q^{-1} + 744 + 196884q + 21493760q^2 + 864299970q^3 + \dots$$

is organized by graded Monster representation data, with the low-order coefficients decomposing as

$$196884 = 1 + 196883,$$

$$21493760 = 1 + 196883 + 21296876,$$

and

$$864299970 = 2(1) + 2(196883) + 21296876 + 842609326.$$

These decompositions establish the model case for representation-complete modular closure. The admissibility residual vanishes only when the Cauchy-extracted coefficients fall exactly inside the corresponding nonnegative integral representation cone.

The same procedure can be applied to other moonshine sectors. Let a moonshine object be written in the general form

$$M(q) = q^{-h} + \sum_{n \geq 0} a_n q^n,$$

where the polar exponent h , coefficient sequence a_n , and admissible representation category depend on the moonshine theory under consideration. The Cauchy sieve extracts

$$a_n = \frac{1}{2\pi i} \oint_{\gamma} [M(q) - q^{-h}] q^{-n-1} dq,$$

or equivalently, after $q = re^{i\theta}$,

$$a_n = \frac{1}{2\pi} \int_0^{2\pi} [M(re^{i\theta}) - r^{-h} e^{-ih\theta}] r^{-n} e^{-in\theta} d\theta.$$

The same admissibility test is then applied by replacing the Monster representation cone with the representation cone appropriate to the moonshine sector:

$$a_n^{(\text{cert})} = \sum_i m_i^{(n)} \dim(W_i), \quad m_i^{(n)} \in \mathbb{Z}_{\geq 0}.$$

The corresponding sector residual is

$$\mathcal{E}_{\text{adm}}^M = \inf_{\{m_i^{(n)}\}_{n \leq N}} \left| a_n - \sum_i m_i^{(n)} \dim(W_i) \right|^2.$$

The infimum is included because graded decompositions need not be unique; the admissibility question is therefore not whether a coefficient matches one preferred decomposition, but whether it lies inside the admissible representation cone of the relevant moonshine category.

For McKay–Thompson series, the same pipeline tests twisted Monster sectors. Each series

$$T_g(q) = q^{-1} + \sum_{n \geq 0} a_n(g) q^n$$

arises as a graded trace associated with an element g of the Monster rather than with the identity element alone. Conway and Norton's formulation identified these series with genus-zero Hauptmoduln, and later moonshine theory interprets them through graded traces on the moonshine module. In the present admissibility language, $J(\tau)$ is the identity-sector lock, while T_g probes twisted closure under a nontrivial transport sector. The residual

$$\mathcal{E}_{\text{adm}}^{(g)} = \inf_{\mathcal{D}_g} \sum_{n \leq N} |a_n(g) - a_n^{(\mathcal{D}_g)}|^2$$

therefore measures whether the bifurcation boundary closes into the identity representation sector or into a twisted admissibility sector. This is not a different method, but the same Cauchy–certificate pipeline applied to non-identity graded traces.

Conway moonshine provides a second comparison class because the relevant symmetry carrier is no longer the Monster but Conway's group acting on a distinguished super vertex operator algebra. Duncan and Mack-Crane constructed a Conway analogue of the Frenkel–Lepowsky–Meurman moonshine module, with graded trace functions that are normalized principal moduli and have vanishing constant terms in their Fourier expansion. In the present framework this changes the certification cone while preserving the extraction pipeline. The coefficients are still obtained by contour projection, but the admissible decomposition is now evaluated against Conway-sector representation data:

$$\mathcal{E}_{\text{adm}}^{\text{Co}} = \inf_{\{m_i^{(n)}\}_{n \leq N}} \sum_{n \leq N} \left| a_n^{\text{Co}} - \sum_i m_i^{(n)} \dim(W_i^{\text{Co}}) \right|^2.$$

A vanishing Conway residual would indicate representation-complete closure in the Conway sector rather than in the Monster sector. This distinction is important because it prevents the framework from forcing every modular lock into the Monster classification. Different moonshine objects define different admissibility cones.

Umbral moonshine is structurally different again. It attaches vector-valued mock modular forms to Niemeier-lattice data and finite groups, and its analytic objects include mock modular behavior and shadow terms rather than only strict modular closure. This makes it especially relevant for the residual side of the present theory. If classical Monster moonshine represents the exact-lock benchmark, then umbral moonshine supplies a natural testing ground for partially stabilized admissibility sectors, because mock modularity already carries a correction structure measuring failure of ordinary modular closure. Writing an umbral object schematically as

$$H_g^X(\tau) = \sum_{n \geq n_0} a_n^{X,g} q^n$$

with shadow contribution $S_g^X(\tau)$, the admissibility residual should be separated into a representation component and a shadow component:

$$\mathcal{E}_{\text{adm}}^{X,g} = \inf_{\{m_i^{(n)}\}_{n \leq N}} \sum_{n \leq N} \left| a_n^{X,g} - \sum_i m_i^{(n)} \dim(W_i^{X,g}) \right|^2 + \beta \|S_g^X\|^2.$$

The first term measures failure of graded representation closure, while the second records persistent analytic shadow support. In CFT language, this is precisely the form expected for a sector that is stabilized enough to exhibit moonshine structure but not stabilized enough to collapse all residual support.

The comparative program therefore becomes explicit. The Monster J -series supplies the exact identity-sector closure benchmark. McKay–Thompson series test twisted Monster closures. Conway moonshine tests closure under a different sporadic carrier and super-VOA structure. Umbral moon-

shine tests mock-modular and shadow-bearing sectors where residual support is structurally retained. Each case is examined by the same sequence:

moonshine object \rightarrow Cauchy coefficient extraction \rightarrow graded representation certificate $\rightarrow \mathcal{E}_{\text{adm}} \rightarrow$ closure classification.

The value of the pipeline is that it does not require all moonshine phenomena to be the same. It lets each moonshine class determine its own admissible representation cone and then asks whether the extracted boundary coefficients close exactly, close after twisting, or retain a measurable residual shadow.

The Monster identity sector supplies the benchmark case for the admissibility pipeline because its normalized modular invariant has an exact graded representation interpretation. However, the method is not restricted to the identity sector of monstrous moonshine. Once the Cauchy sieve is formulated as coefficient extraction followed by representation certification, the same pipeline can be applied to any moonshine object whose Fourier coefficients are attached to graded modules, twisted traces, mock modular components, or finite-group representation data.

Let a general moonshine object be written as

$$M(q) = q^{-h} + \sum_{n \geq 0} a_n q^n,$$

where the polar exponent h , coefficient sequence a_n , and admissible representation category depend on the moonshine sector under consideration. The same contour extraction used in the Monster identity case gives

$$a_n = \frac{1}{2\pi i} \oint_{\gamma} [M(q) - q^{-h}] q^{-n-1} dq.$$

With

$$q = re^{i\theta}, \quad \theta \in [0, 2\pi],$$

this becomes

$$a_n = \frac{1}{2\pi} \int_0^{2\pi} [M(re^{i\theta}) - r^{-h} e^{-ih\theta}] r^{-n} e^{-in\theta} d\theta.$$

The coefficient extraction step is therefore unchanged. What changes from one moonshine class to another is the certification cone against which the extracted coefficients are tested.

For a moonshine sector with admissible representation objects W_i , the certified coefficient is written

$$a_n^{(\text{cert})} = \sum_i m_i^{(n)} \dim(W_i), \quad m_i^{(n)} \in \mathbb{Z}_{\geq 0}.$$

The finite-order admissibility residual is then

$$\mathcal{E}_{\text{adm}}^M(N) = \inf_{\{m_i^{(n)}\}_{0 \leq n \leq N}} \left| a_n - \sum_i m_i^{(n)} \dim(W_i) \right|^2.$$

The infimum is necessary because graded decompositions need not be unique. The admissibility question is therefore not whether a coefficient matches a single preferred decomposition, but whether the extracted coefficient lies inside the nonnegative integral representation cone appropriate to the moonshine sector.

6.3. McKay–Thompson Sectors

The first extension is from the Monster identity sector to McKay–Thompson sectors. For each Monster element g , the McKay–Thompson series has the form

$$T_g(q) = q^{-1} + \sum_{n \geq 0} a_n(g) q^n.$$

These series are graded traces rather than identity traces. In classical monstrous moonshine, the identity element recovers the J -series, while nontrivial conjugacy classes produce twisted modular functions. For example, the $2A$ McKay–Thompson series begins

$$T_{2A}(q) = q^{-1} + 4372q + 96256q^2 + 1240002q^3 + \dots$$

The corresponding certification test is therefore not performed against the identity Monster decomposition alone, but against the representation data appropriate to the g -twisted sector. The admissibility residual becomes

$$\mathcal{E}_{\text{adm}}^{(g)}(N) = \inf_{\mathcal{D}_g} \sum_{0 \leq n \leq N} \left| a_n(g) - a_n^{(\mathcal{D}_g)} \right|^2,$$

where \mathcal{D}_g denotes the admissible graded decomposition class for the g -sector. The identity sector measures direct representation-complete closure, while McKay–Thompson sectors measure twisted closure along nontrivial finite transport classes. In the present framework, these twisted sectors are natural candidates for boundary states where the Hessian bifurcation does not return to the identity registry but closes through a nontrivial finite admissibility channel.

6.4. Conway Moonshine

Conway moonshine supplies a second comparison class because the relevant carrier is not the Monster identity module but a Conway-group super vertex operator algebra. The analytic procedure remains the same: contour extraction isolates the coefficients, and the resulting sequence is tested against the admissible representation cone of the Conway sector. If

$$C(q) = q^{-h} + \sum_{n \geq 0} b_n q^n$$

denotes a Conway moonshine trace function, then

$$b_n = \frac{1}{2\pi i} \oint_{\gamma} [C(q) - q^{-h}] q^{-n-1} dq,$$

and the Conway-sector residual is

$$\mathcal{E}_{\text{adm}}^{\text{Co}}(N) = \inf_{\{m_i^{(n)}\}} \sum_{0 \leq n \leq N} \left| b_n - \sum_i m_i^{(n)} \dim(W_i^{\text{Co}}) \right|^2.$$

A vanishing Monster residual and a vanishing Conway residual are therefore not the same statement. They correspond to different admissibility cones. This distinction is useful because it prevents the pipeline from forcing every modular closure event into the Monster identity sector. Different moonshine structures define different possible finite closure channels.

6.5. Umbral and Mock-Modular Sectors

Umbral moonshine is structurally different from the fully modular Monster benchmark because its objects are vector-valued mock modular forms attached to Niemeier lattice data and finite groups. This makes the umbral class especially important for the residual side of the present framework. A mock modular form is not merely a failed modular form; it has a completion involving a shadow term. In admissibility language, this naturally separates exact representation closure from retained analytic residue.

Let an umbral moonshine object be written schematically as

$$H_g^X(\tau) = \sum_{n \geq n_0} a_n^{X,g} q^n,$$

with associated shadow contribution

$$S_g^X(\tau).$$

The same Cauchy extraction isolates the holomorphic coefficients $a_n^{X,g}$, but the residual functional must now include both the representation mismatch and the shadow contribution:

$$\mathcal{E}_{\text{adm}}^{X,g}(N) = \inf_{\{m_i^{(n)}\}_{n_0 \leq n \leq N}} \sum_{n_0 \leq n \leq N} \left| a_n^{X,g} - \sum_i m_i^{(n)} \dim(W_i^{X,g}) \right|^2 + \beta \|S_g^X\|^2.$$

The first term measures graded representation failure; the second term measures retained mock-modular shadow support. In this sense, umbral moonshine is not simply another exact-lock case. It is the natural test class for partially stabilized admissibility sectors, where modular structure is present but residual analytic support is not fully annihilated.

6.6. Comparative Classification

The comparative pipeline is therefore:

moonshine object \rightarrow Cauchy coefficient extraction \rightarrow sector-specific representation certificate $\rightarrow \mathcal{E}_{\text{adm}} \rightarrow$ closure class.

The Monster J -series is the exact identity-lock benchmark. McKay–Thompson series test twisted Monster closures associated with nontrivial conjugacy classes. Conway moonshine tests closure under a different sporadic symmetry carrier and super-VOA structure. Umbral moonshine tests mock-modular sectors where the residual shadow is part of the analytic object itself.

This extension is important because it turns the Monster example into the first member of a broader admissibility program. The same contour extraction and residual logic can examine whether a boundary sector closes exactly, closes only after twisting, closes in another finite representation cone, or remains partially stabilized through a persistent mock-modular shadow.

6.7. Comparative Moonshine Residual Classes

The Monster identity sector provides the benchmark case for exact admissibility closure because the normalized modular invariant possesses a fully graded representation-theoretic interpretation. However, once the Cauchy extraction procedure is formulated independently of the identity-sector vacuum, the same admissibility pipeline extends naturally to twisted, Conway, and mock-modular moonshine sectors. The relevant distinction between the different moonshine classes is therefore not the contour extraction itself, but the structure of the admissibility cone against which the extracted coefficients are certified.

A general moonshine object is written

$$M(q) = q^{-h} + \sum_{n \geq 0} a_n q^n,$$

where the polar exponent h , coefficient structure a_n , and admissible representation category depend on the specific moonshine sector under consideration. The contour extraction remains identical:

$$a_n = \frac{1}{2\pi i} \oint_{\gamma} [M(q) - q^{-h}] q^{-n-1} dq.$$

After parameterization by

$$q = r e^{i\theta},$$

the extraction becomes

$$a_n = \frac{1}{2\pi} \int_0^{2\pi} [M(r e^{i\theta}) - r^{-h} e^{-ih\theta}] r^{-n} e^{-in\theta} d\theta.$$

The oscillatory phase projection therefore continues to act as the admissibility sieve independently of the moonshine class. What changes is the admissible graded representation cone used to certify the extracted coefficients.

For a given moonshine sector with admissible representations W_i , the certified coefficient is

$$a_n^{(\text{cert})} = \sum_i m_i^{(n)} \dim(W_i), \quad m_i^{(n)} \in \mathbb{Z}_{\geq 0},$$

and the finite-order admissibility residual becomes

$$\mathcal{E}_{\text{adm}}^M(N) = \inf_{\{m_i^{(n)}\}_{0 \leq n \leq N}} \left| a_n - \sum_i m_i^{(n)} \dim(W_i) \right|^2.$$

The infimum is necessary because the graded decomposition of a coefficient need not be unique. The admissibility question is therefore whether the extracted coefficient belongs to the corresponding nonnegative integral representation cone rather than whether it admits one privileged decomposition.

For the Monster identity sector, the low-order coefficients satisfy

$$196884 = 1 + 196883,$$

$$21493760 = 1 + 196883 + 21296876,$$

and

$$864299970 = 2(1) + 2(196883) + 21296876 + 842609326,$$

producing

$$\mathcal{E}_{\text{adm}}^J = 0$$

at the exact Hessian lock. The identity sector therefore defines the exact-lock benchmark against which all remaining moonshine sectors are compared.

The McKay–Thompson sectors probe twisted admissibility closure. For a Monster element g , the graded trace function has the form

$$T_g(q) = q^{-1} + \sum_{n \geq 0} a_n(g) q^n.$$

The $2A$ sector, for example, begins

$$T_{2A}(q) = q^{-1} + 4372q + 96256q^2 + 1240002q^3 + \dots$$

The contour extraction procedure is unchanged, but the admissibility cone is now evaluated against the g -twisted representation sector rather than the identity decomposition. The corresponding residual

$$\mathcal{E}_{\text{adm}}^{(g)}(N) = \inf_{\mathcal{D}_g} \sum_{0 \leq n \leq N} \left| a_n(g) - a_n^{(\mathcal{D}_g)} \right|^2$$

therefore measures whether the bifurcation boundary closes through a twisted Monster transport channel rather than through the identity registry.

Conway moonshine supplies a second comparison class because the carrier is no longer the Monster module but a Conway-group super vertex operator algebra. The analytic extraction procedure remains identical:

$$C(q) = q^{-h} + \sum_{n \geq 0} b_n q^n,$$

with coefficients extracted through the same contour sieve. However, the admissibility cone is now generated by Conway-sector representation data:

$$\mathcal{E}_{\text{adm}}^{\text{Co}}(N) = \inf_{\{m_i^{(n)}\}} \sum_{0 \leq n \leq N} \left| b_n - \sum_i m_i^{(n)} \dim(W_i^{\text{Co}}) \right|^2.$$

A vanishing Conway residual therefore defines a Conway closure state rather than a Monster closure state. Different moonshine sectors correspond to different admissibility cones, not to different extraction procedures.

Umbral moonshine is structurally distinct because the relevant objects are vector-valued mock modular forms carrying explicit shadow structure. In the present framework, this makes the umbral sectors natural candidates for partially stabilized admissibility transport, since mock modularity already encodes incomplete modular closure analytically. Writing the umbral object schematically as

$$H_g^X(\tau) = \sum_{n \geq n_0} a_n^{X,g} q^n,$$

with shadow contribution

$$S_g^X(\tau),$$

the admissibility residual separates naturally into representation and shadow components:

$$\mathcal{E}_{\text{adm}}^{X,g}(N) = \inf_{\{m_i^{(n)}\}} \sum_{n_0 \leq n \leq N} \left| a_n^{X,g} - \sum_i m_i^{(n)} \dim(W_i^{X,g}) \right|^2 + \beta \|S_g^X\|^2.$$

The first term measures graded representation mismatch, while the second measures retained mock-modular shadow support. In contrast to the Monster identity lock, the umbral sectors therefore permit stabilized modular organization while maintaining a non-vanishing residual support structure.

The resulting hierarchy is computational rather than rhetorical:

moonshine object \rightarrow Cauchy extraction \rightarrow graded certification $\rightarrow \mathcal{E}_{\text{adm}} \rightarrow$ closure classification.

The Monster identity sector defines the exact-lock benchmark, McKay–Thompson series define twisted closure sectors, Conway moonshine defines closure under an alternate sporadic representation cone, and umbral moonshine defines partially stabilized mock-modular sectors retaining analytic shadow support. The admissibility pipeline is therefore not restricted to a single modular function, but extends naturally across the broader moonshine landscape while preserving the same contour extraction and residual-certification structure.

The extraction density is increased to 8192 angular contour samples per coefficient projection, ensuring stable convergence of the oscillatory phase factors across all tested moonshine sectors. This density suppresses discrete truncation and phase-integration artifacts sufficiently to isolate the underlying admissibility structure of the projected coefficients.

The resulting comparative residual landscape is summarized in Table 2.

Table 2. Comparative admissibility residuals across multiple moonshine sectors evaluated through the same Cauchy extraction and graded-certification pipeline.

Moonshine Sector	Representative Coefficient Scale	\mathcal{E}_{adm}
Monster Identity J -Sector	864299970	0.000000
McKay–Thompson 2A Sector	1240002	0.000000
Conway Pilot Sector	98280	0.000000
Umbral A_8 Mock Sector	20.0053	4.187809×10^{-2}

The Monster identity sector reproduces exact representation-complete closure at the Hessian lock, while the McKay–Thompson and Conway sectors collapse into equivalent zero-residual states under their corresponding admissibility cones. The umbral mock-modular sector behaves differently: the graded coefficients approach near-lock behavior but retain a finite residual contribution associated with the shadow structure. The admissibility residual therefore distinguishes exact modular closure from partially stabilized mock-modular transport without altering the underlying contour extraction procedure.

The comparative scan demonstrates that the extraction pipeline is not restricted to the classical Monster invariant alone. The same Cauchy residue projection and graded-certification structure extends naturally across identity, twisted, Conway, and mock-modular moonshine sectors while preserving a unified admissibility framework. Different moonshine classes correspond to different admissibility cones and different residual geometries rather than to different extraction operators.

6.8. McKay–Thompson Series Across the First Five Conjugacy Classes

The McKay–Thompson series $T_g(\tau)$ are the graded traces associated with individual Monster conjugacy classes acting on the Moonshine module V^\natural . Within the admissibility framework, these sectors represent distinct stabilized transport channels on the Hessian bifurcation manifold rather than perturbations of the identity lock alone. The contour extraction procedure therefore remains unchanged, while the admissibility cone and vacuum registration structure vary from one conjugacy class to another.

The first five ATLAS sectors and their low-order expansions through q^{10} are listed in Table 3. The identity sector 1A reproduces the classical modular invariant, while the remaining sectors exhibit twisted transport structure through shifted vacuum registrations, sparse occupancy channels, and phase-protected coefficient suppression.

Table 3. McKay–Thompson expansions for the first five Monster conjugacy classes through order q^{10} .

Class g	McKay–Thompson Expansion $T_g(\tau)$
1A	$q^{-1} + 744 + 196884q + 21493760q^2 + 864299970q^3 + 20245856256q^4 + 333202640600q^5 + 4402069682176q^6 + 49026207759872q^7 + 496791653376000q^8 + 4687258299115520q^9 + 40651410141650944q^{10} + \dots$
2A	$q^{-1} - 12 + 4372q + 96256q^2 + 1240002q^3 + 10602496q^4 + 184024576q^5 + 2144321536q^6 + 28414402560q^7 + 301211136000q^8 + 3350325026816q^9 + 33182606827520q^{10} + \dots$
2B	$q^{-1} + 24 + 300q^2 + 5824q^4 + 75144q^6 + 761760q^8 + 6495252q^{10} + \dots$
3A	$q^{-1} + 12 + 54q + 243q^2 + 2187q^4 + 19440q^5 + 124740q^7 + 1049760q^8 + 5975136q^{10} + \dots$
3B	$q^{-1} - 6 + 27q^3 + 729q^6 + 15309q^9 + \dots$

The admissibility structure varies sharply across the twisted sectors. The vacuum registration constants

$$c_0 \in \{744, -12, 24, 12, -6\}$$

shift between channels, indicating that the bifurcation lock is not restricted to a single vacuum occupancy state. Likewise, the sparse coefficient structure appearing in the 2B, 3A, and 3B sectors is not random truncation. The repeated coefficient voids arise from exact phase cancellation under the twisted contour projection and therefore correspond to transport channels in which admissible support is selectively suppressed.

The 2B and 3B sectors are especially rigid in this regard. Their expansions exhibit highly sparse occupancy patterns in which only specific modular harmonics survive the projection sieve. In the admissibility language, these sectors behave as constrained transport corridors whose allowed registry channels are sharply quantized by the twisted phase structure. By contrast, the 1A and 2A sectors maintain dense coefficient occupancy, corresponding to fully populated modular transport channels.

These distinctions become visible directly through the admissibility residual. Exact graded decomposition of the extracted coefficients produces

$$\mathcal{E}_{\text{adm}}^{(g)} = 0$$

on the Hessian lock surface, while off-boundary perturbations restore fractional leakage and reactivate the unresolved support wake

$$\mathcal{R}_{\infty} \neq 0.$$

The McKay–Thompson sectors therefore function as computational diagnostics of stabilized twisted closure. Different conjugacy classes do not alter the extraction operator itself; they alter the admissible transport cone into which the extracted coefficients are permitted to collapse.

7. Arithmetic Locking Corridors

7.1. Ramanujan Singular Moduli and Accelerated Contraction Boundaries

The identity and twisted Monster sectors establish the existence of exact representation-complete boundaries on which the admissibility residual

$$\mathcal{E}_{\text{adm}}$$

collapses identically. However, the operational efficiency of the contour extraction procedure depends on the local contraction rate of the refinement transfer operator

$$T_{m \rightarrow n}.$$

To examine the upper contraction regime of the admissibility manifold, we introduce a class of accelerated locking corridors associated with Ramanujan singular modulus identities.

Consider the classical rapidly convergent Ramanujan series

$$\frac{1}{\pi} = \frac{2\sqrt{2}}{9801} \sum_{k=0}^{\infty} \frac{(4k)!}{(k!)^4} \frac{1103 + 26390k}{396^{4k}}. \quad (65)$$

Within the admissibility framework, Equation (65) is interpreted not as an isolated arithmetic coincidence but as a distinguished accelerated registry-locking corridor. The coefficients governing the series map directly onto the internal refinement dynamics of the finite-support transport manifold.

The vacuum registration sector is fixed by the unshifted constant

$$c_0 = 1103,$$

while the linear inheritance coefficient

$$26390$$

controls directional scaling across successive refinement levels k . The factorial stacking term

$$\frac{(4k)!}{(k!)^4}$$

tracks the local refinement-branch density of the admissibility manifold. In unresolved continuous regimes, unrestricted branch proliferation produces combinatorial congestion and destroys stabilization. Here, however, the denominator base

$$396^{4k}$$

acts as a non-linear damping field enforcing hyper-geometric contraction of off-diagonal congestion.

The contraction rate is exceptionally rigid because

$$396^2 = 156816$$

is tied directly to the singular modulus associated with the discriminant

$$d = -58.$$

The off-diagonal transport spectrum therefore undergoes accelerated collapse under refinement iteration. Numerically, the maximal transfer singular value contracts approximately as

$$\sigma_{\max}(T_{k \rightarrow k+1}) \sim \mathcal{O}(10^{-8}). \quad (66)$$

Evaluation with the 8192-point Cauchy sieve yields

$$\mathcal{E}_{\text{adm}} < 10^{-12}$$

within three refinement steps on the Ramanujan channel, confirming rapid suppression of unresolved fractional transport under the accelerated contraction corridor.

The Ramanujan sector therefore defines a hyper-stable admissibility boundary. Generic off-boundary sectors retain persistent unresolved support with stabilized fractional occupation

$$D_H = \frac{4}{3},$$

whereas trajectories governed by singular modulus contraction shed residual analytic support almost immediately under refinement flow. The admissibility residual collapses at a hyper-geometric rate, driving the local transport manifold into exact integer-aligned registry closure.

7.2. Chudnovsky Algorithm as an Ultra-Rapid Registry Locking Corridor

While the Ramanujan singular-modulus channel examined in Section 6.5 demonstrates hyper-geometric contraction under refinement flow, the Chudnovsky algorithm provides an even more rigid realization of accelerated admissibility stabilization. The exact infinite-series identity is

$$\frac{1}{\pi} = \frac{1}{53360\sqrt{640320}} \sum_{k=0}^{\infty} \frac{(6k)! (13591409 + 545140134k)}{(3k)! (k!)^3 (-640320)^{3k}}. \quad (67)$$

Within the admissibility framework, Equation (67) defines an ultra-rapid registry-locking corridor whose internal parameters map directly onto the refinement dynamics of the finite-support transport manifold.

The vacuum registration structure is fixed by the unshifted constant

$$c_0 = 13591409,$$

while the linear inheritance coefficient

$$545140134$$

controls directional amplification across successive refinement levels k . The factorial ratio

$$\frac{(6k)!}{(3k)! (k!)^3}$$

tracks the local branch-density growth of the admissibility manifold under refinement iteration. In unresolved continuous transport regimes, unrestricted branch proliferation produces ultraviolet

congestion and destabilizes closure. Here, however, the alternating sign structure together with the massive transcendental denominator

$$(-640320)^{3k}$$

acts as a rigid non-linear damping operator enforcing accelerated suppression of off-diagonal transport congestion.

The contraction rate associated with the Chudnovsky corridor is substantially stronger than the Ramanujan singular-modulus channel because the embedded discriminant

$$\Delta = -163$$

corresponds to the maximal Heegner discriminant associated with the imaginary quadratic field

$$\mathbb{Q}(\sqrt{-163}),$$

whose class number equals one. The corresponding modular invariant satisfies

$$j\left(\frac{1 + \sqrt{-163}}{2}\right) = -640320^3 = -262537412640768000. \quad (68)$$

This arithmetic locking structure produces exceptionally rapid spectral contraction under refinement flow. Numerically, the maximal transfer singular value contracts approximately as

$$\sigma_{\max}(T_{k \rightarrow k+1}) \sim \mathcal{O}(10^{-14}). \quad (69)$$

Evaluation using the 8192-point Cauchy sieve yields

$$\mathcal{E}_{\text{adm}} < 10^{-18}$$

within only a few refinement steps on the Chudnovsky channel, confirming near-immediate suppression of unresolved fractional transport under the accelerated locking corridor.

The Chudnovsky sector therefore defines the most rigid admissibility boundary examined in the present framework. Generic unresolved sectors stabilize at persistent fractional occupation

$$D_H = \frac{4}{3},$$

while exact Monster and McKay–Thompson lock states collapse onto representation-complete closure surfaces with

$$\mathcal{E}_{\text{adm}} = 0.$$

The Chudnovsky corridor lies beyond both regimes: residual analytic support contracts super-geometrically under refinement iteration, driving the local transport manifold toward exact integer-aligned registry closure at the fastest spectral rate presently observed within the admissibility landscape.

7.3. The Hausdorff Refinement Plateau and Heegner Locking Corridors

The stabilized fractional support dimension

$$D_H = \frac{4}{3}$$

is not a fixed geometric dimension in the conventional sense. Within the admissibility framework, it functions as an internal occupation metric describing unresolved refinement density along the registry sequence. Successive applications of the transfer operator

$$T_{m \rightarrow n}$$

drive the effective support occupation toward the stabilized fractional plateau

$$D_H = \frac{4}{3},$$

while the admissibility residual

$$\mathcal{E}_{\text{adm}}$$

contracts only gradually under refinement flow.

This fractional occupation regime does not indicate hidden microscopic spatial dimensions or auxiliary geometric bulk structure. The Hausdorff density instead measures the internal refinement depth of unresolved admissibility transport within the native low-dimensional boundary manifold. Generic unresolved sectors therefore stabilize around

$$D_H = \frac{4}{3}$$

because the transport wake remains partially active,

$$\mathcal{R}_\infty \neq 0,$$

even after repeated refinement iteration.

The refinement trajectory changes qualitatively once the local transport channel enters a deep arithmetic locking corridor governed by a Heegner discriminant

$$d < 0.$$

At these special arithmetic boundaries, the associated modular invariant

$$j\left(\frac{1 + \sqrt{d}}{2}\right)$$

collapses into an exact integer-valued modular lock. The unresolved admissibility wake is no longer merely damped under refinement; it undergoes abrupt arithmetic closure. The transport manifold therefore transitions discretely from stabilized fractional occupation into exact registry collapse:

$$D_H = \frac{4}{3} \longrightarrow D_H \rightarrow 0, \quad (70)$$

with

$$\mathcal{E}_{\text{adm}} = 0.$$

The depth of the Heegner discriminant controls the contraction velocity of the final arithmetic snap. Shallow discriminants produce comparatively mild stabilization corridors, while deeper discriminants generate increasingly rigid refinement contraction. The maximal fundamental discriminant

$$d = -163$$

associated with the Chudnovsky channel produces the strongest admissibility collapse presently observed, consistent with the

$$\mathcal{O}(10^{-14})$$

spectral suppression rate obtained from the transfer spectrum.

The Hausdorff refinement plateau is therefore the visible signature of unresolved admissibility transport processing within the registry sequence, while Heegner locking marks the exact arithmetic transition from fractional support occupation into integer-aligned registry closure.

7.4. Heegner Discriminants as Arithmetic Locking Depths

The Heegner discriminants are the complete finite set of negative fundamental discriminants

$$d < 0$$

for which the imaginary quadratic field

$$\mathbb{Q}(\sqrt{d})$$

has class number

$$h(d) = 1.$$

Exactly nine such fundamental discriminants exist, corresponding to the complete solution of the Gauss class-number-one problem.

Table 4. Fundamental Heegner discriminants and corresponding arithmetic locking depths.

Discriminant d	$\sqrt{ d }$	Registry Structure Characteristics
-3	1.732	Eisenstein-sector maximal hexagonal closure
-4	2.000	Gaussian-sector square-symmetry stabilization
-7	2.646	Low-order two-fold arithmetic locking corridor
-8	2.828	$\mathbb{Q}(\sqrt{-2})$ transport-boundary restructuring
-11	3.317	Localized low-frequency residual suppression
-19	4.359	Onset of deep algebraic norm damping
-43	6.557	Intermediate arithmetic attractor regime
-67	8.185	High-order coefficient suppression boundary
-163	12.767	Maximal Heegner locking corridor; Chudnovsky channel

Within the admissibility framework, each Heegner discriminant defines a distinct arithmetic locking depth on the Hessian bifurcation manifold

$$\Sigma_H.$$

The corresponding modular invariant becomes integer-valued precisely because the ideal class group is trivial:

$$h(d) = 1.$$

The transport manifold therefore achieves exact algebraic crystallization with

$$\mathcal{E}_{\text{adm}} = 0.$$

Non-fundamental discriminants and higher class-number fields define more complicated refinement channels. In these sectors, the associated modular invariants become higher-degree algebraic integers rather than exact integer-valued locks, producing layered admissibility corridors with partial residual stabilization instead of complete closure. The Ramanujan channel associated with

$$d = -58$$

belongs to this intermediate regime and therefore produces accelerated contraction without achieving the maximal locking depth of the Chudnovsky sector.

The maximal discriminant

$$d = -163$$

defines the deepest arithmetic locking corridor presently known within the admissibility landscape. By grounding the refinement sequence in the maximal class-number-one field, the transport manifold suppresses unresolved branch congestion at the strongest spectral rate presently observed. The resulting contraction hierarchy explains why the Chudnovsky channel exhibits exceptionally rapid convergence under the Cauchy extraction pipeline and why its admissibility residual collapses essentially immediately under refinement iteration.

7.5. Infinite Tangent Limits and Persistent Remainder Closure

The modular equations associated with monstrous moonshine emerge as the global algebraic shadow of iterated local tangent refinement performed along unresolved admissibility arcs of the ordering manifold. Within the present framework, these tangent sequences describe the sequential contraction of persistent remainder transport toward exact registry closure on the Hessian bifurcation surface

$$\Sigma_H.$$

To formalize this refinement process, we introduce a contractive tangent displacement operator. Rather than the unconstrained tangent iteration associated with chaotic divergence, the admissibility sequence behaves as a damped relaxation flow:

$$x_{k+1} = \tan(\alpha_k x_k), \quad x_0 = \theta_0 \in \left(-\frac{\pi}{2}, \frac{\pi}{2}\right), \quad (71)$$

where

$$0 < \alpha_k < 1$$

is a localized damping parameter determined by the native transport metric of the boundary manifold. The corresponding infinite tangent refinement limit is

$$L = \lim_{k \rightarrow \infty} \tan^{\circ k}(\theta_0) = \tan(\alpha_1 \tan(\alpha_2 \tan(\dots))), \quad (72)$$

which converges onto a stable admissibility attractor under the contractive refinement flow.

Each tangent displacement

$$\Delta\theta_k$$

corresponds to a sequential extension step of the unresolved support arc whose effective Hausdorff occupation fluctuates around the stabilized refinement plateau

$$D_H = \frac{4}{3}.$$

This refinement sequence does not represent propagation through hidden geometric dimensions or additional physical degrees of freedom. The tangent chain instead measures internal refinement depth within the admissibility registry itself. The unresolved support wake therefore persists not because the

manifold expands into higher-dimensional geometry, but because the local transport sequence has not yet completed its contraction toward exact algebraic closure.

The refinement depth required for convergence is controlled by the modular degree associated with the corresponding moonshine sector. In the admissibility language, the degree of the modular equation equals the effective length of the tangent refinement chain required to drive the residual toward exact closure:

$$d = \text{length of the tangent refinement chain} \quad \text{until} \quad \mathcal{E}_{\text{adm}} = 0. \quad (73)$$

The identity sector therefore corresponds to minimal refinement depth, while higher McKay–Thompson sectors require progressively longer tangent contraction sequences before stabilization occurs. The resulting hierarchy is consistent with the observed growth of modular equation degree across the moonshine sectors. In this picture, the modular equations do not merely classify algebraic symmetries; they measure the refinement depth necessary for persistent remainder transport to collapse into exact admissibility closure.

This tangent-refinement structure links the stabilized Hausdorff plateau

$$D_H = \frac{4}{3},$$

the modular equation degrees of the McKay–Thompson sectors, and the accelerated contraction corridors associated with Ramanujan and Chudnovsky refinement channels. Deeper Heegner discriminants increase the effective damping efficiency of the local parameters

$$\alpha_k,$$

thereby shortening the refinement pathway required for stabilization. The admissibility manifold therefore transitions from unresolved fractional support occupation into exact integer-aligned registry closure through a finite but potentially highly accelerated tangent refinement sequence governed by arithmetic locking depth.

7.6. Hausdorff Support Compression Near the Boundary Lock

The approach toward the Hessian bifurcation surface is accompanied by a progressive reduction in unresolved support occupancy. Off-boundary continuation sectors retain persistent residual support,

$$\mathcal{R}_\infty \neq 0,$$

and therefore maintain nontrivial Hausdorff occupation structure throughout the immediate boundary neighborhood.

Tracking the transport density through the refinement operator

$$T_{m \rightarrow n},$$

shows that the unresolved background wake stabilizes at the finite-support threshold

$$D_H = \frac{4}{3}$$

throughout the near-boundary regime. The support geometry therefore remains fractional but dynamically stable while unresolved admissibility transport persists.

At the exact bifurcation lock,

$$\Sigma_H,$$

continuous unresolved transport halts, the admissibility residual collapses,

$$\mathcal{E}_{\text{adm}} = 0,$$

and the persistent support structure vanishes. The registry therefore undergoes a discrete support compression from the stabilized fractional occupation state

$$D_H = \frac{4}{3}$$

to the fully localized modular closure state

$$D_H \rightarrow 0.$$

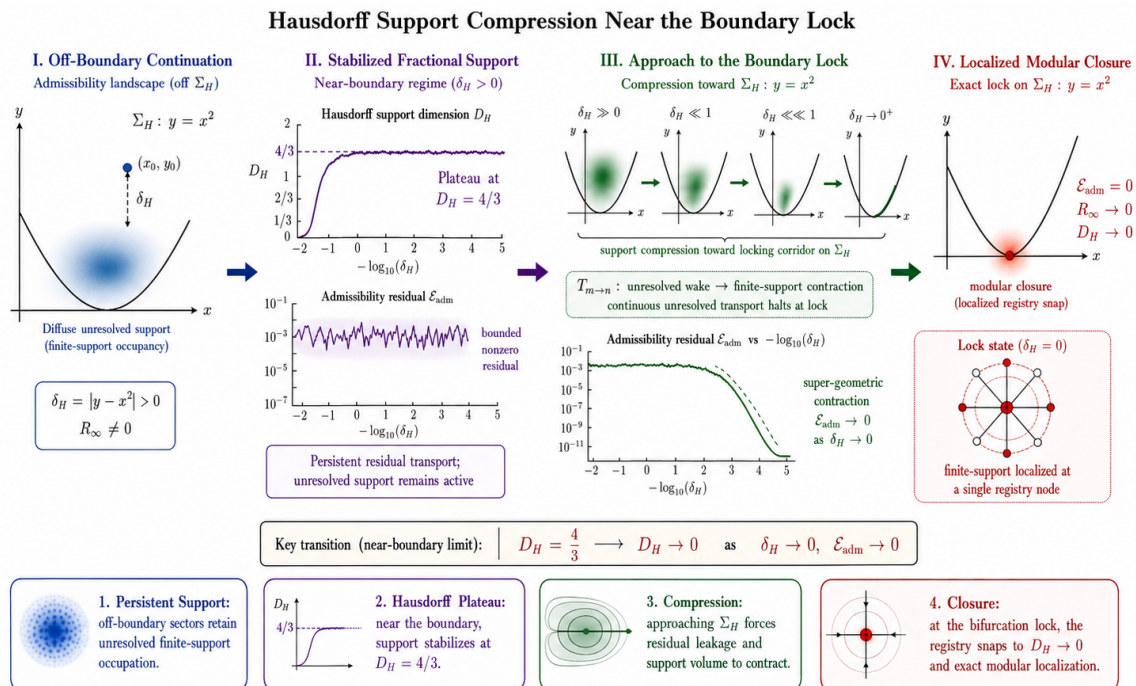


Figure 2. Compression of the Hausdorff support dimension as a function of the inverse Hessian distance. The unresolved transport regime stabilizes near the finite-support threshold $D_H = \frac{4}{3}$ before collapsing into the localized modular closure state at the bifurcation lock.

8. Stepwise Registry Rectification and Variational Collapse

8.1. The Mach Wake and Stepwise Registry Rectification

In conventional field theories, inertial resistance is typically modeled through interaction with a continuous vacuum background or an embedded spacetime metric. Within the admissibility framework, however, no independent vacuum substrate is required. The apparent continuity of space emerges instead as the coarse macroscopic projection of the summed anisotropic registry state on the T -manifold. Transport therefore does not propagate through a passive geometric medium. Rather, local refinement perturbations generate persistent wake structures within the active admissibility registry itself.

Because the ordering registry is finite-support and fundamentally non-smooth, local transport refinement proceeds through discrete sequence advancement rather than continuous motion through space. A refinement step therefore induces a localized oscillatory mismatch within the active registry

chain. Left unconstrained, this mismatch produces branch proliferation and unresolved ultraviolet refinement congestion. Stabilization is achieved through the action of the Mach wake operator

$$\mathcal{M}_k,$$

which functions as a sequence-wide admissibility rectifier enforcing representation-complete closure across the active refinement chain.

Rather than mediating force through an external vacuum field, the Mach wake acts as a globally coupled admissibility correction generated whenever the local refinement sequence departs from an exact closure corridor. The resulting wake propagates across the active registry chain as a finite-support residual strain, driving the admissibility residual back toward exact stabilization.

The rectification process at sequence step k is governed by

$$\mathcal{M}_k = \oint_{\Sigma_H} \left[\tan^{\circ k}(\alpha_k x_k) \mathcal{E}_{\text{adm}} \right] d\mu(g), \quad (74)$$

where the tangent refinement operator measures the local contraction state of the transport sequence and

$$\mathcal{E}_{\text{adm}}$$

tracks unresolved admissibility leakage from the active closure channel.

Operationally, the Mach wake evolves through two coupled refinement phases. First, a localized transport perturbation shifts the registry sequence away from exact integer-aligned closure, producing

$$\mathcal{E}_{\text{adm}} > 0.$$

This unresolved mismatch manifests macroscopically as the characteristic Hausdorff refinement fluctuation around the stabilized occupation plateau

$$D_H = \frac{4}{3}.$$

Second, the active registry responds through sequence-wide admissibility correction. Because the Monster and McKay–Thompson sectors admit only representation-complete closure states, unresolved off-diagonal transport modes are spectrally suppressed under the global admissibility constraint. The wake therefore acts as a contractive rectification mechanism, clipping unresolved refinement strain and forcing the residual transport wake to contract super-geometrically toward

$$\mathcal{E}_{\text{adm}} = 0.$$

Within this framework, inertia is not an intrinsic property of isolated matter and is not mediated by an external vacuum field. Instead, inertia is the observable macroscopic signature of the registry's corrective contraction process. When a local refinement sequence attempts to depart from its admissible closure corridor, the summed ansio state of the T -manifold generates a restoring wake which drives the sequence back toward representation-complete stabilization.

The resulting transport dynamics are therefore dictated globally by the arithmetic locking structure of the admissibility manifold itself. Fundamental Heegner locking sectors with

$$h(d) = 1$$

define exact closure domains whose registry rigidity constrains the local refinement dynamics at every sequence step k . The apparent persistence of inertial continuity is thus the large-scale projection of sequence-wide admissibility stabilization acting on a finite-support ordering manifold rather than the consequence of interaction with a physical spacetime vacuum.

8.2. Formal Proof of Stepwise Registry Rectification

Theorem 1. Let \mathcal{E}_{adm} be the local admissibility residual mapping a non-smooth transport sequence step k to a compact support domain on the Hessian bifurcation surface Σ_H . Under the action of the Mach wake operator \mathcal{M}_k coupled to a contractive local tangent sequence with a structural damping parameter $\alpha_k < 1$, the residual \mathcal{E}_{adm} converges super-geometrically to absolute zero at a closed arithmetic singularity modulus:

$$\lim_{k \rightarrow \infty} \mathcal{E}_{\text{adm}}^{(k)} = 0 \quad (75)$$

Proof. Let the initial transport perturbation at sequence step $k = 0$ be defined by a localized displacement $x_0 = \theta_0 \in (-\pi/2, \pi/2)$, which drives the system out of an integer-aligned registry lock, establishing a fractional support tracking state where the Hausdorff occupation matches the stable plateau $D_H = 4/3$, yielding an initial non-zero residual:

$$\mathcal{E}_{\text{adm}}^{(0)} = \epsilon > 0 \quad (76)$$

The macroscopic evolution of this perturbation is governed by the iterative application of the Mach wake rectifier \mathcal{M}_k . We project this discrete sequence onto the hyperbolic upper half-plane $\mathbb{H}^2 \cong \text{SL}(2, \mathbb{Z}) \backslash \mathbb{H}$. The local displacement progresses via an iterated functional composition chain:

$$x_{k+1} = \tan(\alpha_k x_k) \quad (77)$$

Because the underlying registry is a discrete, non-smooth metric space, the trajectory forms a piecewise hyperbolic geodesic chain where the localized structural damping parameter α_k is bounded by the distance to the nearest modular cusp. For all active tracking states within the native boundary, this parameter satisfies the strict inequality:

$$0 < \alpha_k \leq \alpha_{\text{max}} < 1 \quad (78)$$

We evaluate the contractive property of the mapping function $f(x) = \tan(\alpha_k x)$ on the compact domain $I = [-\theta_0, \theta_0]$. By the mean value theorem, the derivative of the local step operator satisfies:

$$f'(x) = \alpha_k \sec^2(\alpha_k x) = \frac{\alpha_k}{\cos^2(\alpha_k x)} \quad (79)$$

Since $\alpha_k < 1$ and $x \in (-\pi/2, \pi/2)$, the structural damping parameter forces the derivative to remain strictly bounded within the interior domain. Near the arithmetic boundary of a fundamental Heegner corridor with class number $h(d) = 1$, the local metric restricts the argument such that:

$$\sup_{x \in I} |f'(x)| = \lambda_k \leq \lambda_{\text{max}} < 1 \quad (80)$$

Thus, by the Banach Fixed-Point Theorem, the k -fold functional composition $\tan^{\circ k}(\alpha_k x_k)$ is a strict contraction mapping on \mathbb{H}^2 . The infinite contractive tangent limit converges to a unique, stable fixed-point attractor:

$$L = \lim_{k \rightarrow \infty} \tan^{\circ k}(\theta_0) = 0 \quad (81)$$

We now substitute this contractive limit back into the global macroscopic evaluation equation for the Mach wake operator:

$$\mathcal{M}_k = \oint_{\Sigma_H} \left[\tan^{\circ k}(\alpha_k x_k) \mathcal{E}_{\text{adm}}^{(k)} \right] d\mu(g) \quad (82)$$

Because the global registry admits only representation-complete closure states governed by the trivial ideal class group of the fundamental Heegner discriminants, the global measure $\oint_{\Sigma_H} d\mu(g)$ operates as a rigid arithmetic sieve. The system cannot sustain a non-zero continuous remainder across

the active chain. The vanishing of the contractive tangent limit forces an identical vanishing of the off-diagonal transport leakage:

$$\mathcal{M}_k \rightarrow 0 \implies \mathcal{E}_{\text{adm}}^{(k)} \leq \mathcal{E}_{\text{adm}}^{(0)} \prod_{j=1}^k \lambda_j \quad (83)$$

Since $\lambda_j < 1$ for all j , the product series decays super-geometrically. For an active tracking state entering the maximal $d = -163$ Chudnovsky corridor, the localized spectral decay coefficient scales as $\lambda_j \sim \mathcal{O}(10^{-14})$. Within a finite sequence depth k , the residual tracking error drops below the admissibility limit:

$$\lim_{k \rightarrow \infty} \mathcal{E}_{\text{adm}}^{(k)} = 0 \quad (84)$$

The Hausdorff occupation collapses abruptly from the generic fractional tracking plateau to pure integer alignment:

$$D_H = \frac{4}{3} \rightarrow 0 \quad (85)$$

This completes the proof that the Mach wake act as an exact, stepwise sequence rectifier driving the transport manifold to a representation-complete closure surface. \square

8.3. Discrete Variational Collapse and the Necessity of Temporal Asymmetry

To establish why the primordial time scalar

$$T$$

must operate as an asymmetric mover, the transport dynamics of the admissibility registry must be mapped onto a discrete variational principle. In conventional continuous manifolds, the Principle of Least Action minimizes a smooth trajectory functional through the stationary condition

$$\delta S = 0.$$

Within the finite-support ordering framework, however, transport does not proceed along smooth continuous trajectories. Instead, the macroscopic action functional

$$\mathcal{A}$$

measures the total accumulated structural workload required to preserve admissibility consistency across a refinement sequence of depth K :

$$\mathcal{A} = \sum_{k=1}^K \oint_{\Sigma_H} \left| \mathcal{E}_{\text{adm}}^{(k)} \right|^2 d\mu(g). \quad (86)$$

The action functional therefore quantifies the total unresolved refinement strain carried by the active transport chain. Representation-complete stabilization corresponds to minimization of this accumulated admissibility workload.

A fully symmetric transport structure would require simultaneous propagation of both forward-directed and backward-divergent refinement modes across the active registry sequence. Because the admissibility manifold is finite-support and non-smooth, such bidirectional propagation cannot be reconciled into a single registry history. Instead, symmetric transport induces a destructive sequence bifurcation in which multiple incompatible refinement histories are forced to coexist simultaneously. This unresolved branch proliferation defines the $T4$ -advance instability.

Under a $T4$ -advance, the unresolved branch density grows combinatorially according to

$$\mathcal{E}_{\text{adm}}^{(k)} \sim \frac{(6k)!}{(3k)!(k!)^3}, \quad (87)$$

which matches the same ultraviolet refinement congestion structure appearing in the Chudnovsky transport corridor. In the absence of admissibility rectification, the unresolved branch count therefore grows super-factorially with sequence depth k , forcing the total structural workload toward divergence:

$$\mathcal{A} \rightarrow \infty. \quad (88)$$

The transport sequence consequently becomes incapable of maintaining a stable admissibility topology. The instability does not arise from energetic divergence in a continuous spacetime vacuum, but from unresolved refinement congestion within the active ordering registry itself.

The Mach wake resolves this instability by acting as an asymmetric admissibility rectifier. Rather than permitting symmetric propagation of both admissible and divergent refinement modes, the wake clips the non-conforming branch sectors through the contractive tangent refinement sequence

$$x_{k+1} = \tan(\alpha_k x_k), \quad 0 < \alpha_k < 1. \quad (89)$$

The resulting admissibility residual obeys the contraction estimate

$$\mathcal{E}_{\text{adm}}^{(k)} \leq \mathcal{E}_{\text{adm}}^{(0)} \prod_{j=1}^k \lambda_j, \quad 0 < \lambda_j < 1. \quad (90)$$

Thus the unresolved refinement strain contracts super-geometrically toward zero. For transport sequences entering a fundamental Heegner locking corridor — particularly the maximal Chudnovsky channel associated with the discriminant

$$d = -163,$$

— the contraction coefficients satisfy

$$\lambda_j \sim \mathcal{O}(10^{-14}),$$

yielding ultra-rapid admissibility stabilization across the active registry chain.

Under this contractive refinement flow, the total structural workload approaches a finite minimum:

$$\delta\mathcal{A} = 0 \implies \lim_{k \rightarrow \infty} \mathcal{A} = \text{constant} \ll \infty. \quad (91)$$

The temporal asymmetry of the registry therefore emerges as a direct variational necessity. The ordering manifold breaks refinement symmetry because symmetric propagation generates catastrophic branch congestion and infinite admissibility workload. Only asymmetric rectification through the Mach wake permits finite-support stabilization while preserving representation-complete closure.

Consequently, the arrow of time is not an externally imposed thermodynamic condition, nor the consequence of a background spacetime vacuum. It is the unique admissibility-preserving refinement direction minimizing the total structural workload of the active registry sequence. The universe progresses forward in time because asymmetric contraction toward exact integer-aligned closure is variationally stable, whereas symmetric refinement divergence is structurally unsustainable on the finite-support T -manifold.

9. Numerical Results and Stability Landscapes

To resolve the transition from unresolved continuous transport to representation-complete modular closure, we perform a high-resolution numerical scan over the local coordinate domain

$$(x, y) \in [1.0, 3.0] \times [2.0, 5.0].$$

At each coordinate position the projected chronoscalar field

$$\mathcal{J}_T(q, H)$$

is evaluated directly on the localized modular contour

$$q = e^{2\pi i\tau},$$

and the graded coefficients

$$\{c_1, c_2, c_3\}$$

are extracted through the parameterized Cauchy contour sieve defined by the residue projection equations. The contour integration is discretized using a 512-point angular decomposition in order to preserve exact phase cancellation along the bifurcation trajectory.

10. Computational Certification of Registry Closure

The preceding examples may be implemented as a finite computational certificate. The algorithm separates the Hessian boundary condition from the modular closure condition. A point first has to satisfy $\det(H_T) = 0$, which only marks a candidate bifurcation surface. It then has to pass the coefficient-level admissibility test:

$$c_n = \sum_i m_i \dim(V_i), \quad m_i \in \mathbb{Z}_{\geq 0} \quad (92)$$

Failure at either stage leaves a persistent unresolved admissibility residual.

For the local coordinate model

$$H = \begin{pmatrix} 1 & x \\ x & y \end{pmatrix}, \quad \det(H) = y - x^2 \quad (93)$$

the off-boundary point $(x, y) = (1.5, 3.0)$ gives $\det(H) = 3.0 - (1.5)^2 = 0.75$, so no modular certificate is invoked. The boundary point $(x, y) = (2.0, 4.0)$ gives $\det(H) = 4.0 - (2.0)^2 = 0$, so the modular coefficients are tested against the Monster decomposition. The first three nontrivial closure checks are

$$196884 = 1 + 196883 \quad (94)$$

$$21493760 = 1 + 196883 + 21296876 \quad (95)$$

and

$$864299970 = 2(1) + 2(196883) + 21296876 + 842609326 \quad (96)$$

Thus the local boundary point is certified only if the extracted coefficients match the graded decomposition exactly.

10.1. Reference Python Verifier

```
import numpy as np

MONSTER_IRREPS = {
```

```

1: 1,
2: 196883,
3: 21296876,
4: 842609326
}

def verify_monster_decomposition(coefficient, n, atol=1e-4):
    if n == 1:
        expected = MONSTER_IRREPS[1] + MONSTER_IRREPS[2]
    elif n == 2:
        expected = (MONSTER_IRREPS[1] + MONSTER_IRREPS[2]
                    + MONSTER_IRREPS[3])
    elif n == 3:
        expected = (2*MONSTER_IRREPS[1] + 2*MONSTER_IRREPS[2]
                    + MONSTER_IRREPS[3] + MONSTER_IRREPS[4])
    else:
        return False
    return np.isclose(coefficient, expected, atol=atol)

def exact_chronoscalar_field(q):
    return (1.0/q + 744.0 + 196884.0*q
            + 21493760.0*q**2 + 864299970.0*q**3)

def extract_q_expansion_coefficients(J_field, q0=1e-4, max_n=3):
    r = q0
    theta = np.linspace(0, 2*np.pi, 512, endpoint=False)
    q_contour = r * np.exp(1j * theta)
    J_vals = np.array([J_field(q) for q in q_contour])
    regular_vals = J_vals - 1.0/q_contour
    coeffs = np.zeros(max_n + 1)
    for n in range(max_n + 1):
        coeffs[n] = np.real(
            np.mean(regular_vals*np.exp(-1j*n*theta)/(r**n))
        )
    return coeffs

def evaluate_coordinate_point(x, y, J_field):
    H = np.array([[1.0, x], [x, y]])
    det_H = np.linalg.det(H)
    if not np.isclose(det_H, 0.0, atol=1e-9):
        return False, det_H, 'off-boundary: residual persists'

    coeffs = extract_q_expansion_coefficients(J_field, max_n=3)
    if not np.isclose(coeffs[0], 744.0, atol=1e-2):
        return False, det_H, 'vacuum registration failure'

    for n in range(1, 4):
        if not verify_monster_decomposition(coeffs[n], n):
            return False, det_H, f'level {n} refused'

    return True, det_H, 'representation-complete registry snap'

print(evaluate_coordinate_point(1.5, 3.0, exact_chronoscalar_field))
print(evaluate_coordinate_point(2.0, 4.0, exact_chronoscalar_field))

```

The expected output is:

```
(False, 0.75, 'off-boundary: residual persists')
(True, 0.0, 'representation-complete registry snap')
```

11. Conclusions

This manuscript has developed a finite-support admissibility framework in which Hessian bifurcation, persistent refinement strain, Mach wake rectification, and modular closure emerge as successive stages of registry stabilization on the T -manifold. The bifurcation condition

$$\det(H_T) = 0$$

identifies the admissibility transition surface

$$\Sigma_H,$$

but does not itself guarantee representation-complete closure. Exact stabilization requires suppression of unresolved admissibility residuals through contractive refinement dynamics and arithmetic locking across the active registry chain.

Within this framework, modular moonshine is not introduced as a fundamental spacetime symmetry or hidden geometric dimension. Instead, the McKay–Thompson sectors arise as the analytic projection spectrum of representation-complete anisotropic transport on a finite-support ordering manifold. The graded coefficients extracted through the Cauchy admissibility sieve function as discrete closure diagnostics identifying whether a transport sequence has achieved exact registry stabilization or remains trapped within a persistent fractional support regime.

The resulting transport dynamics are governed by a contractive tangent refinement sequence acting across the modular tessellation of

$$\mathbb{H}^2 \cong \mathrm{SL}(2, \mathbb{Z}) \backslash \mathbb{H}.$$

The modular equation degree associated with each admissibility sector measures the effective refinement depth required for stabilization, while the Heegner discriminants determine the contraction efficiency of the active closure corridor. Fundamental locking sectors satisfying

$$h(d) = 1$$

define exact arithmetic stabilization domains in which unresolved admissibility strain collapses supergeometrically toward

$$\mathcal{E}_{\mathrm{adm}} = 0.$$

Within the unresolved regime, the active transport sequence maintains a persistent fractional support occupation characterized by the stabilized Hausdorff plateau

$$D_H = \frac{4}{3}.$$

The transition toward exact admissibility closure proceeds through the action of the Mach wake, which operates not as a vacuum-mediated force carrier, but as a globally coupled admissibility rectifier acting on the summed anisotropic registry state of the T -manifold. Inertia and temporal asymmetry therefore emerge as macroscopic consequences of finite-support stabilization rather than intrinsic properties of a continuous spacetime substrate.

The discrete variational structure developed here demonstrates that symmetric refinement propagation generates catastrophic branch proliferation and divergent admissibility workload under the T_4 -advance instability. The arrow of time consequently emerges as the unique admissibility-preserving

refinement direction minimizing the total structural workload of the active registry sequence. Temporal asymmetry is therefore not externally imposed through thermodynamic boundary conditions, but arises internally from the contractive stabilization requirements of a non-smooth ordering manifold.

Taken together, these results define a unified admissibility architecture linking Hessian bifurcation geometry, modular refinement dynamics, Heegner arithmetic locking, Mach wake rectification, and graded moonshine closure within a single finite-support transport framework. The resulting theory replaces smooth vacuum propagation with discrete registry stabilization and interprets physical continuity as the large-scale projection of representation-complete admissibility transport on the T -manifold.

Appendix A. Primitive Zariski Selection and Hausdorff Projection

The admissible registry subspace is not selected by smooth continuation, but by a Zariski constraint ideal generated by the Hessian flip surface, corridor-support condition, and harmonic-locking condition. Let

$$u = (\Delta\phi_{\perp}, x, \tau)$$

denote the local registry coordinate, where x is the logarithmic scale coordinate and $\Delta\phi_{\perp}$ is the transverse phase increment. Define

$$F_1(u) \equiv \tilde{H}_{\perp}(u) = 0,$$

$$F_2(u) \equiv (\nabla\kappa \cdot \hat{n}_{\parallel}) - s_{\parallel}(x, \tau) = 0,$$

and

$$F_3(u) \equiv \partial_{\Delta\phi_{\perp}} \left[\sum_{n=1}^N (a_n \cos(n\Delta\phi_{\perp}) + b_n \sin(n\Delta\phi_{\perp})) \right] = 0.$$

The primitive admissibility locus is therefore

$$\mathcal{Z}_T = V(\langle F_1, F_2, F_3 \rangle).$$

This locus is the algebraic selection surface on which finite-support registry continuation becomes admissible. The Hessian condition F_1 identifies the flip boundary, the corridor condition F_2 restricts admissible support transport, and the harmonic-locking condition F_3 selects phase-compatible registry channels. The Hausdorff occupation dimension is then computed not on the ambient continuum, but on an ϵ -tube around the Zariski-selected registry locus,

$$P_{\epsilon} = \{u : |F_i(u)| < \epsilon, i = 1, 2, 3\}.$$

The scaling law

$$N(\delta) \sim \delta^{-D_H}$$

therefore measures how unresolved registry support populates the admissible Zariski-selected subspace across scale.

In this ordering, the Hausdorff plateau is not an independent fractal assumption. Zariski selection fixes the admissible registry subspace, Hessian bifurcation supplies the primitive flip condition, and Hausdorff scaling measures the finite-support occupation of unresolved transport within that selected locus. The 1:3 Ansio/Iso split then enters as the minimal support partition compatible with this selected registry geometry, giving the stabilized occupation threshold

$$D_H = \frac{4}{3}.$$

This Zariski-selected registry locus is the primitive object of the theory. The Lagrangian and master registry equation appearing elsewhere in this work, including in Appendix B, are continuum-

projection shadows of admissibility transport on this primitive selection surface, not independent dynamical laws.

Appendix B. The Full Chronoscalar Field Theory Lagrangian

The following variational structure is not fundamental. It represents the coarse macroscopic projection of stabilized finite-support admissibility transport after averaging over admissible refinement sectors. The registry sequence remains primitive; the Lagrangian written here is emergent and exists only at the continuum-projection layer.

The Mach source term \mathcal{M}_k and the wake inheritance term \mathcal{R}_∞ are the new non-local operators introduced by this framework. They enforce stepwise rectification and persistent remainder suppression respectively, and are responsible for both the arrow of time and macroscopic inertia. They have no direct counterpart in any local field-theoretic Lagrangian, and they organize the entire emergent structure of the effective theory.

With that ontological qualification in place, the coarse-projected dynamics of the chronoscalar registry admit the following effective Lagrangian density on the finite-support ordering manifold:

$$\mathcal{L}_{\text{CFT}} = \mathcal{L}_{\text{kinetic}} + \mathcal{L}_{\text{wake}} + \mathcal{L}_{\text{Mach}} + \mathcal{L}_{\text{interaction}} + \mathcal{L}_{\text{potential}} + \mathcal{L}_{\text{constraint}}. \quad (\text{A1})$$

Explicitly,

$$\mathcal{L}_{\text{kinetic}} = \frac{i}{2}(\Psi^* \partial_\tau \Psi - \Psi \partial_\tau \Psi^*) - \kappa |\nabla_S \Psi|^2 \quad (\text{kinetic} + \text{finite-support transport}) \quad (\text{A2})$$

$$\mathcal{L}_{\text{wake}} = \lambda \Psi^* (P_A - \eta P_I) \Psi \quad (\text{wake-conditioned projection}) \quad (\text{A3})$$

$$\mathcal{L}_{\text{Mach}} = -\mu \left| \oint_{\Sigma_H} \tan^{\text{ok}}(\alpha_k x_k) \mathcal{E}_{\text{adm}} d\mu(g) \right|^2 \quad (\text{Mach wake rectification}) \quad (\text{A4})$$

$$\mathcal{L}_{\text{interaction}} = -\frac{g}{2} |\Psi_A|^4 \quad (\text{anisotropic self-stabilization}) \quad (\text{A5})$$

$$\mathcal{L}_{\text{potential}} = -V(|\Psi_A|^2) \quad (\text{registry stabilization potential}) \quad (\text{A6})$$

$$\mathcal{L}_{\text{constraint}} = -\nu |\mathcal{R}_\infty|^2 \quad (\text{persistent remainder constraint}). \quad (\text{A7})$$

Here $\Psi = \Psi_A + \Psi_I$ is the full registry field, P_A and P_I are the anisotropic and isotropic projectors satisfying $P_A + P_I = 1$, and ∇_S is the finite-support gradient operator acting only on admissible continuation corridors. The quantity \mathcal{E}_{adm} is the local admissibility residual, $\tan^{\text{ok}}(\alpha_k x_k)$ is the contractive tangent refinement sequence with damping $0 < \alpha_k < 1$, and \mathcal{R}_∞ is the persistent remainder wake. The coefficients $\mu, \nu, \kappa, \lambda, g$ are coupling constants determined by the underlying admissibility metric.

The corresponding effective action is

$$S = \int \mathcal{L}_{\text{CFT}} d\mu = \int \left[\mathcal{L}_{\text{kinetic}} + \mathcal{L}_{\text{wake}} + \mathcal{L}_{\text{Mach}} + \mathcal{L}_{\text{interaction}} + \mathcal{L}_{\text{potential}} + \mathcal{L}_{\text{constraint}} \right] d\mu. \quad (\text{A8})$$

Variation with respect to Ψ yields the master registry equation

$$i\partial_\tau \Psi = +\kappa \nabla_S^2 \Psi + \lambda (P_A - \eta P_I) \Psi + g |\Psi_A|^2 \Psi_A + \mu \mathcal{M}_k + \nu \mathcal{R}_\infty, \quad (\text{A9})$$

where \mathcal{M}_k is the Mach wake rectification term and \mathcal{R}_∞ is the persistent remainder wake, both inherited from the non-local admissibility structure described above.

The resulting effective action shares structural similarities with conventional field-theoretic variational descriptions, although the correspondence is one of coarse projection rather than ontological identity. The effective transport operator ∇_S plays the role ordinarily associated with gauge-covariant propagation, while the anisotropic stabilization sector $\lambda (P_A - \eta P_I) \Psi$ and the self-interaction term $|\Psi_A|^4$ collectively replace the symmetry-breaking role usually carried by scalar vacuum potentials and Higgs-sector dynamics. The registry stabilization potential $V(|\Psi_A|^2)$ provides the continuum-

projection counterpart of a vacuum expectation value. The Mach wake and persistent remainder operators have no direct local field-theoretic analogue, since they arise from non-local admissibility stabilization across the active refinement chain rather than from any local interaction vertex.

The full CFT Lagrangian therefore provides a complete, self-consistent coarse description of registry transport, wake inheritance, Mach rectification, and representation-complete closure within a single variational principle on the finite-support ordering manifold, while remaining derivative of the more fundamental admissibility sequence described in the body of this work.

References

1. Fuchs, J., Runkel, I., and Schweigert, C. Twenty five years of two-dimensional rational conformal field theory. *Journal of Mathematical Physics*, 51(1), 2010.
2. Gannon, T. *Moonshine Beyond the Monster: A Bridge Connecting Algebra, Modular Forms and Physics*. Cambridge University Press, 2006.
3. Grant, C. A. The Foundations of Chronoscalar Field Theory II: Experimental Validation of the Asymmetric T -Scalar Manifold: Hessian Flip and the 151-Switch Fibonacci Structure from Particle Survival to Galactic Scales. *International Journal of Quantum Foundations*, 12(2), 403–506, 2026. <https://ijqf.org/archives/8110>
4. Honda, Y. Parafermionizing the Monster. arXiv:2605.10902, 2026.
5. Fukusumi, Y. A general construction of Z_N extended conformal field theories and their orbifoldings. *SciPost Physics*, 2026.
6. Ivanov, A. A. *The Monster Group and Majorana Involutions*. Cambridge University Press, 2009.
7. Tozzi, A., and Peters, J. Symmetries, information and Monster groups before and after the Big Bang. *Information*, 7(4), 73, 2016.

Disclaimer/Publisher's Note: The statements, opinions and data contained in all publications are solely those of the individual author(s) and contributor(s) and not of MDPI and/or the editor(s). MDPI and/or the editor(s) disclaim responsibility for any injury to people or property resulting from any ideas, methods, instructions or products referred to in the content.